On modelling exothermic/endothermic phase transformations in shape memory alloys

Cristian FĂCIU and **Mihaela MIHĂILESCU-SULICIU**
Institute of Mathematics of the Romanian Academy
P.O. Box 1-764, Bucharest, Romania

Abstract

We present an overview of a recent one-dimensional rate-type viscoelastic model for shape memory alloys and its predictions for strain controlled problems. The model is based on a rate-type thermo-viscoelastic constitutive relation. Its equilibrium stress-strain-temperature response is a non-monotone stress-strain relation for certain ranges of temperature. Each domain of convexity is identified with a phase (or variant of phase) of the material. The numerical simulations successfully capture the nucleation and evolution of transformation fronts and the corresponding temperature fields observed in laboratory experiments. The number of nucleation events and kinetics of transformation fronts were found to be sensitive to the imposed loading rate due to the release/absorbtion of latent heat. We also show that the pseudoelastic hysteresis in their strain-stress curves increases when the imposed rate is increased.

Keywords: Non-convex free energy; Phase transition; Austenite; Martensite; Constitutive behavior; Thermo-viscoelasticity.

1 Introduction

Shape memory alloys (SMA) and their two unusual characteristics: the pseudoelastic hysteresis and the shape memory effect have received sustained attention in recent years (see for instance Otsuka and Wayman, (1998)). The shape memory effect is the material's ability to recover at zero stress large mechanically-induced strains (up to 8%) by moderate increases in temperature ($\approx 10-20^0C$). Pseudoelasticity refers to the materials's ability in a somewhat higher temperature regime to be strained significantly (to strains higher than 6%) and return to its unstrained configuration upon unloading via a hysteresis loop. The underlying mechanism is a reversible transformation between two solid state phases called *austenite* (A) and *martensite* (M) often occurring near room temperature. The transformation can be stress-induced or temperature-induced causing a strong thermo-mechanical coupling in the material behavior. These properties have been discovered half a century ago, but the interest in these alloys has recently increased and stems in part from their applicability as elements in active structure.

Many micromechanical aspects of SMA's behavior have been elucidated during the 40-years history of SMAs and there is a rich material science literature on this subject (see for instance Perkins (1975); Otsuka et al. (1976); Shaw and Kyriakides (1995) and the literature therein). Since the special properties of SMAs make it a promising candidate for novel structural applications simple continuum models which allow to capture the main micromechanical features observed in laboratory experiments are required. The last two decades have seen some notable constitutive modelling efforts. We mention here only some of these approaches as for instance Tanaka et al. (1986), Ball and James (1987), Abeyaratne and Knowles (1993), Battacharya and Kohn (1996), Brinson (1993), Bruno (1995), Leo et al. (1993), Shaw and Kyriakides (1998, 2000).

A classical constitutive viewpoint in studying phase transforming materials is based on the thermoelasticity theories with multiple energy-wells and started at the end of XIX century with the equation of van der Waals for thermoelastic fluids. In these theories each energy-well is identified with a phase of the material. In solid mechanics such an approach, which is equivalent with non-monotone stress-strain relation for certain ranges of temperature, has been initiated by Ericksen (1975) in an isothermal and one-dimensional context and was followed by numerous and important studies. Some of them (see for instance James (1981, 1983), Ball and James (1987)) appeal to the minimization of the stored energy of the mixed phases and use sophisticated mathematical techniques in variational calculus. In fact, these studies do not address the *process* of phase transformation that leads to inelastic behavior rather they investigate the coexistence of the phases after the transformation has taken place. Thus these studies are concerned to find out the amount of phases that coexist and the way in which they are juxtaposed (at a very fine scale) to achieve a known macroscopic shape. It is important to recognize that the response of the final state with mixed (and constant) phases is *elastic* for a certain range of deformations. It is this observation that justifies appealing to the minimization of the stored energy, as is usually done in classical elasticity.

The merit of these studies consist in the understanding of equilibrium martensitic microstructure and its relation to basic crystallography. Much, however, remains unknown concerning the nucleation and evolution of microstructure, and the resultant hysteresis. In fact the notion that distinguishes inelastic materials from elastic materials is that of "dissipation".

It is thus obvious that in the frame of elasticity with multiple stored energy-wells there is a deficiency of constitutive information. It is known that this deficiency also leads to ill-posed problems in the sense of Hadamard when we consider initial-boundary value problems for the corresponding field of equations. To overcome this inconveniency some authors have developed some theories which explicitly account for dissipation. For example Rajagopal and Srinivasa (1995) have proposed a criterion based on energetics for the initiation and propagation of twinning; Abeyaratne and Knowles (1993) have developed a thermodynamical framework based on the concept of driving force and in addition to the usual thermoelastic properties they introduced a nucleation criterion and a kinetic relation for the motion of interfaces.

A different approach to the problem of phase transformation or strain localization in materials exhibiting material instabilities has been advanced in the context of a van der Waals fluid by Suliciu (1989) (see also Făciu, 1991; Suliciu, 1992), but this method can be applied to elastic bars as well. This formulation is based on a rate-type viscoelastic constitutive equation with Maxwellian viscosity. In fact one augments the conventional constitutive law for an elastic material capable of undergoing phase transitions in such a way that the stress depends not only on the strain, but also on the strain rate and the stress rate. The dependence on strain is non-linear and non-monotone, and the dependence on strain rate and stress rate is linear and is associated with a viscosity coefficient and a linear instantaneous response of the material, respectively. Thus this simple rate-dependent constitutive equation has the capability to describe relaxation, creep and instantaneous processes of the material and moreover it acknowledges (see Mihailescu-Suliciu and Suliciu, 1993; Făciu and Suliciu, 1994; Făciu, 1996) the material instabilities which have been observed (see Shaw and Kyriakides, 1997) in the pseudoelastic behavior of some SMAs as NiTi for instance. Its strain and stress-dependent free energy function is non-convex. In fact this approach is equivalent to a model for a simple body with one internal variable (the inelastic strain). Thus one obtains a viscoelastic approach to non-monotone elasticity which no longer leads to ill posed problems since the corresponding PDEqs system is hyperbolic semilinear. The nucleation and propagation of one phase into another is automatically accounted for in the case of this model and it is explained by a linear stability analysis performed by Suliciu (1992). A detailed investigation on the way the dissipation mechanism included in this model describes the process of nucleation and growth of the phases can be found in Făciu (1996).

It is important to note here that unlike other approaches, which simulate phase transformation in experiments one might normally consider quasistatic (global strain rates less than $10^{-2}/s$), the inertia forces are here taken into account as they play an essential role when instability phenomena accompanying phase transformation processes develop. This is justified by the fact that a phase transition is a process in which a region occupied by one phase grows at the expense of a region occupied by another phase, with the essential physical activity occurring in the neighborhood of the interfaces separating phases, where local dynamic effects appear. As a consequence the Maxwellian approach can successfully capture the "go-and-stop" phase propagation phenomenon, often observed in materials presenting material instabilities which manifest through serrated load-deformation curves in strained controlled experiments.

Recent advances in experimental techniques have been developed by Shaw and Kyriakides, (1997) (see also Leo et al. 1993; Lin et al., 1994;). They allowed access for synchronized optical and infrared imaging of the specimen deformation and temperature fields and have clarified many aspects of the strong coupling between the thermal and mechanical properties of NiTi. Thus the way the exothermic $(A) \rightarrow (M)$ transition during loading tends to cause self-heating and the endothermic $(M) \rightarrow (A)$ transition during unloading causes self-cooling has been associated with the phenomena of initiation and propagation of transformation fronts.

In a recent paper (see Făciu and Mihăilescu-Suliciu (2002a)) we extended the Maxwellian viscoelastic approach in order to include thermal effects accompanying phase transitions in SMAs. We have considered a rate-type semilinear thermo-viscoelastic approach to nonlinear and non-monotone thermoelasticity by taking into account an explicit temperature dependent equilibrium stress-strain relation (see also Suliciu, 1998).

Let us note that a related viscoelastic approach to the isothermal problem of phase transition in solid bodies has been proposed by Pego (1987) for a dead-loading experiment and used by Vainchtein and Rosakis (1999) for strain controlled problems and extended by Vainchtein (2002) for the case of temperature dependent non-monotone equilibrium stress-strain relations. This formulation is based on a Kelvin-Voight viscoelastic model for which the stress depends only on strain and strain rate. This dependence is non-monotone with respect to the strain, but the strain rate enters linearly and is associated with a Newtonian viscosity. As a consequence the model can describe only creep processes, but not relaxation and instantaneous processes and the PDEqs system which describes the motion of a thin bar is parabolic. There are many similarities between the viscoelastic Maxwellian and Newtonian approaches of non-monotone elasticity and an investigation concerning the differences between the predictions of these two models should be made.

The outline of this paper is as follows. We start in Section 2 with a review of the *geometrical* and *kinematical* assumptions for a general formulation of a one dimensional thermomechanical bar theory in a reference configuration. We combine geometrical effects associated with slow variation of cross-sectional area in the case of uniaxial tensile tests with thermomechanical coupling by taking into account the loss of heat across its lateral surface. In Section 3 we formulate the general framework of our constitutive assumptions and we analyse the restrictions imposed on them by the second law of thermodynamics. The free energy of the Maxwell rate-type thermo-viscoelastic constitutive equation is described and some of its properties are surveyed. The relation between our rate-type approach and a constitutive theory with one internal variable is discussed in Section 4. Based on the thermo-mechanical properties of SMAs we consider in Section 5 an explicit equilibrium stress-strain-temperature relation. For this simple case we describe the stress-strain-temperature dependent free energy function of the viscoelastic model as well as its equilibrium entropy and free energy functions. The application of our model for a real experiment is done in Section 6. Here we carry out two numerical simulations of strain-controlled experiments and compare them with the laboratory results obtained by Shaw and Kyriakides (1997).

2 Bar with geometrical defect - a one-dimensional setting

In this section we briefly review some relevant concepts and notations from the continuum theory of thermomechanical processes within a purely one-dimensional setting that corresponds to a uniaxial tensile deformation of a thin rod. We give a general formulation combining the thermomechanical coupling of the material with its environment and geometrical effects associated with the variation of cross-sectional areas.

2.1 Balance equations

Consider a thin bar $\mathcal{B}$ of length L in its unstressed reference configuration, having a variable cross-sectional area along its axis OX. We suppose that the motion of the bar is only longitudinal and it is described by a function

$$x = \chi(X,t), \qquad X \in [0,L], \quad t \geq 0, \tag{1}$$

with the property that for any fixed t, $\chi(X,t)$ is injective and bicontinuous with respect to X. X is the initial axial coordinate, x is the actual axial coordinate and t denotes time. $\chi(\cdot,t)$ is called the *deformation* (or, *configuration*) of the bar $\mathcal{B}$ at time t. Whenever χ is continuously differentiable, we may introduce the functions

$$v(X,t) = \frac{\partial \chi}{\partial t}(X,t), \qquad \varepsilon(X,t) = \frac{\partial \chi}{\partial t}(X,t) - 1 > -1, \tag{2}$$

called the *particle velocity*, and the *strain* respectively at point X and time t.

In the hypothesis of a very small imperfection of the specimen we can neglect some three- dimensional aspects of stress, temperature and strain distribution. Thus we can assume that the only non-zero stress component is the axial stress σ, i.e. the force per unit area in the reference configuration, and all the thermomechanical field quantities are uniform over a cross-section, that is they only depend on X and t.

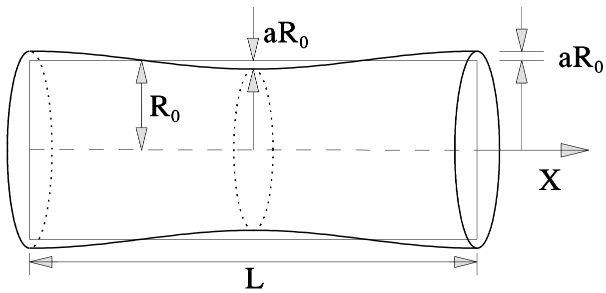

Figure 1: Bar geometry.

A typical example, which will be considered in numerical applications, is the case of a cylindrical bar with a slow variation of its radius $R = R(X)$ along its symmetry axis

$$R(X) = R_o \left(1 + a \sin \pi \left(\frac{1}{2} - \frac{2X}{L}\right)\right), X \in [0,L],$$

where a is a geometric parameter and its value is usually taken between 10^{-1} and 10^{-7}.

Under the above basic assumptions the integral form of the balance of momentum, balance of energy as well as the second law of thermodynamics have to be written as

$$
\begin{aligned}
&\frac{\partial}{\partial t}\int_{X_1}^{X_2} \varrho v A dX = \int_{X_1}^{X_2} \varrho b A dX + \sigma(X_2,t)A(X_2) - \sigma(X_1,t)A(X_1) \\
&\frac{\partial}{\partial t}\int_{X_1}^{X_2} \varrho\left(\frac{v^2}{2}+e\right) A dX = \int_{X_1}^{X_2} \varrho(bv+r) A dX + (\sigma v - q)(X_2,t)A(X_2) \\
&\qquad\qquad\qquad - (\sigma v - q)(X_1,t)A(X_1) + \int_{A_{lat}} \tilde{q} ds, \\
&\frac{\partial}{\partial t}\int_{X_1}^{X_2} \varrho \eta A dX \geq \int_{X_1}^{X_2} \varrho \frac{r}{\theta} A dX - \frac{q}{\theta}(X_2,t)A(X_2) + \frac{q}{\theta}(X_1,t)A(X_1) + \int_{A_{lat}} \frac{\tilde{q}}{\theta} ds,
\end{aligned}
\tag{3}
$$

for any $X_1, X_2 \in [0, L]$ and any $t \in [0, t_0)$.

Here $A = A(X)$ is the *cross-sectional area* of the bar, $\varrho = \varrho(X)$ is the *mass density*, $e = e(X,t)$ is the *internal energy* per unit volume, $\eta = \eta(X,t)$ is the *entropy* per unit volume, $q = q(X,t)$ is the *axial heat flux* across a unit area, $\tilde{q} = \tilde{q}(X,t)$ is the *heat flux across the lateral surface* of the bar per unit area, $b = b(X,t)$ is the *body force* per unit volume, $r = r(X,t)$ is the *heat supply* per unit volume, in the reference configuration, respectively.

When all functions present in (3) are sufficiently smooth we get the local form of the balance equations as

$$
\begin{aligned}
&\varrho\frac{\partial v}{\partial t} - \frac{\partial \sigma}{\partial X} = \varrho b + \frac{A'(X)}{A(X)}\sigma, \\
&\frac{\partial \varepsilon}{\partial t} - \frac{\partial v}{\partial X} = 0, \\
&\varrho\frac{\partial}{\partial t}\left(\frac{v^2}{2}+e\right) = \varrho(bv+r) + \frac{\partial}{\partial X}(\sigma v - q) + \frac{A'(X)}{A(X)}(\sigma v - q) + \frac{2\pi R(X)}{A(X)}\tilde{q}, \\
&\varrho\frac{\partial \eta}{\partial t} \geq \varrho\frac{r}{\theta} - \frac{\partial}{\partial X}\left(\frac{q}{\theta}\right) - \frac{A'(X)}{A(X)}\frac{q}{\theta} + \frac{2\pi R(X)}{A(X)}\frac{\tilde{q}}{\theta},
\end{aligned}
\tag{4}
$$

where we also added the compatibility equation $(4)_2$ between the strain and particle velocity which in the present one-dimensional setting is equivalent to the conservation of mass; we also used $A'(X) \equiv dA(X)/dX$.

As usual, by using $(4)_{1+2}$ into $(4)_3$ and $(4)_4$ we can rewrite the system (4) under the form

$$
\begin{aligned}
&\varrho\frac{\partial v}{\partial t}-\frac{\partial \sigma}{\partial X}=\varrho b+\frac{2R'(X)}{R(X)}\sigma,\\
&\frac{\partial \varepsilon}{\partial t}-\frac{\partial v}{\partial X}=0,\\
&\varrho\frac{\partial e}{\partial t}-\sigma\frac{\partial \varepsilon}{\partial t}+\frac{\partial q}{\partial X}=-\frac{2R'(X)}{R(X)}q+\frac{2}{R(X)}\tilde{q}+\varrho r,\\
&\varrho\theta\frac{\partial \eta}{\partial t}\geq\varrho\frac{\partial e}{\partial t}-\sigma\frac{\partial \varepsilon}{\partial t}+\frac{q}{\theta}\frac{\partial \theta}{\partial X},
\end{aligned}
\tag{5}
$$

where we also have assumed that the bar is circular, i.e. $A(X)=\pi R^2(X)$.

Let us note that the ratio $2R'(X)/R(X)$ has the same order of magnitude as the geometrical parameter a and the corresponding new terms in the balance of momentum and the balance of energy play only the role of a small perturbation.

If we introduce now the (Helmholtz) free energy $\psi=e-\theta\eta$, the second law of thermodynamics $(5)_4$ may also be written in the usual form

$$
\varrho\frac{\partial \psi}{\partial t}\leq\sigma\frac{\partial \varepsilon}{\partial t}-\varrho\eta\frac{\partial \theta}{\partial t}-\frac{q}{\theta}\frac{\partial \theta}{\partial X}. \tag{6}
$$

3 Constitutive assumptions

The system of PDEqs $(5)_{1-3}$ with the unknown functions v, σ, ε, e, q, $\tilde{q}$ which governs the motion of a non-uniform thin rod has to be completed with a set of constitutive equations. Moreover, these constitutive relations have to be compatible with the second law of thermodynamics $(5)_4$ (or (6)) which should ensure the existence of an entropy function η (or, equivalently of a free energy function ψ).

Let us start with the heat flux across the lateral surface of the bar. We suppose in the following that it satisfies a Newton's type convection mode of heat transfer, i.e.

$$
\tilde{q}_{|A_{lat}}=-\omega(\theta_{|A_{lat}}-\theta_{o|A_{lat}})\ ,\ \omega=\text{const.}>0, \tag{7}
$$

where $\theta=\theta(X,t)$ is the *absolute temperature*, $\theta_o=\theta_0(X,t)$ is the *ambient temperature* and ω is a material parameter which characterizes the thermal interaction between the bar and its surroundings.

We consider a *state* of the body any triplet $S = (\chi(X), \sigma(X), \theta(X))$, $X \in [0, L]$ where $\chi(X)$ is a *deformation* of the bar, $\sigma(X)$ and $\theta(X)$ are a stress and temperature field over the body, respectively.

We also assume as given the following set of continuous and piecewise smooth functions $(G, \hat{e}, \hat{\psi}, \hat{\eta}, \hat{q})$ defined on $\mathcal{D} \times R$, where $\mathcal{D} \subset (-1, \infty) \times R \times R^+$ is a constitutive domain in the strain-stress-temperature space, such that

$$\begin{aligned} \frac{\partial \sigma}{\partial t} =& E\frac{\partial \varepsilon}{\partial t} + G(\varepsilon, \sigma, \theta, \theta_X), \\ e =& \hat{e}(\varepsilon, \sigma, \theta, \theta_X), \quad \frac{\partial \hat{e}}{\partial \theta} \neq 0, \\ \psi =& \hat{\psi}(\varepsilon, \sigma, \theta, \theta_X), \text{ or } \eta = \hat{\eta}(\varepsilon, \sigma, \theta, \theta_X), \\ q =& \hat{q}(\varepsilon, \sigma, \theta, \theta_X), \end{aligned} \tag{8}$$

where the material parameter $E = \text{const.} > 0$ is a dynamic Young modulus and the subscript X denotes partial derivative.

A *smooth process* of the bar will be any triplet $S = (\chi(\cdot, X), \sigma(\cdot, X), \theta(\cdot, X))$, $t \in [0, t_0)$ of smooth time dependent fields over $\mathcal{B}$ which satisfies the constitutive equations (7)+(8) and the balance equations $(5)_{1-3}$.

We introduce the following notation for the kernel of the function $G(\varepsilon, \sigma, \theta, g)$

$$\mathcal{E} = \{(\varepsilon, \sigma, \theta, \theta_X) \mid G(\varepsilon, \sigma, \theta, \theta_X) = 0, \quad \text{for } (\varepsilon, \sigma, \theta, \theta_X) \in \mathcal{D} \times R\}$$

. The set $\mathcal{E}$ is called the thermoelastic set, or the *equilibrium set* of the constitutive equation $(8)_1$.

Let us denote by

$$\varepsilon^i = \varepsilon - \frac{\sigma}{E}, \quad \text{and} \quad \varepsilon^e = \frac{\sigma}{E}, \tag{9}$$

the *inelastic strain* and *the elastic strain* at a state S, respectively. Relation $(8)_1$ implies that the inelastic strain of an equilibrium state (i.e. belonging to $\mathcal{E}$) is permanent. Using these notations the constitutive relations (8) may be seen as a constitutive structure for a body with only one internal variable, i.e. the inelastic strain (see Section 4).

The constitutive structure (7) and (8) is said to be compatible with the second law of thermodynamics if there exist a continuous and piecewise smooth entropy function $\eta = \hat{\eta}(\varepsilon, \sigma, \theta, \theta_X)$, $\hat{\eta} : \mathcal{D} \times R \to R$ (or equivalently, a continuous and piecewise smooth free energy function $\psi = \hat{\psi}(\varepsilon, \sigma, \theta, \theta_X)$, $\hat{\psi} : \mathcal{D} \times R \to R$) such that the Clausius-Duhem inequality $(5)_4$ (or (6)) is satisfied (in the points where the derivatives of $\hat{\eta}$, $\hat{\psi}$, $\hat{e}$ make sense) for any smooth process $S = (\varepsilon(\cdot, X), \sigma(\cdot, X), \theta(\cdot, X)) \in \mathcal{D}$, $t \in [0, t_0)$.

In order to exploit the Clausius-Duhem inequality we use now a standard procedure which does not need to define thermodynamic processes by a suitable choice of body forces b and heat supply r (see Coleman and Noll, 1963), but it uses the concept of thermodynamic admissible rates proposed by Suliciu (1983) and used by Făciu (1985). By thermodynamic admissible rates we mean the time derivatives of thermodynamic fields at the initial time, compatible with the general balance laws, with the constitutive assumptions and with the initial conditions of an initial value problem.

We prove that our constitutive structure (7) and (8) admits an entropy function (or, equivalently a free energy function), i.e. it is compatible with the second law of thermodynamics, if and only if the constitutive functions entering (8) satisfy the following conditions

$$\frac{\partial \hat{\psi}}{\partial \theta_X} = 0, \qquad \frac{\partial \hat{\psi}}{\partial \varepsilon} + E\frac{\partial \hat{\psi}}{\partial \sigma} = \frac{\sigma}{\varrho}, \qquad \hat{\eta} = -\frac{\partial \hat{\psi}}{\partial \theta} \tag{10}$$

$$\varrho\frac{\partial \hat{\psi}}{\partial \sigma}G(\varepsilon, \sigma, \theta, \theta_X) + \frac{\hat{q}}{\theta}\theta_X \leq 0, \tag{11}$$

for any $(\varepsilon, \sigma, \theta, \theta_X) \in \mathcal{D} \times R$.

Remark 1. Let us note that, the same as in classical thermodynamic relations, the free energy $\hat{\psi}$ has to be independent on θ_X and it is a potential for the entropy.

Remark 2. The residual inequality (11) contains two terms. The first one is usually associated with the internal dissipation while the second one with the thermal dissipation by heat conduction. Without additional constitutive assumptions nothing can be said about the signs of each of the two quantities.

Remark 3. It is known that the procedure of Coleman and Noll (1963) by which the laws of thermodynamics are used to deduce constitutive restrictions, when applied to the usual forms of the balance laws imposes extraordinarily severe restrictions on the long range spatial dependence allowable for a large class of materials in constitutive quantities. Thus the energy, entropy and stress for the class of deformable elastic bodies could not depend on higher spatial gradients of temperature or higher strain gradients. In the case of our constitutive structure (8) the dissipation inequality (11) allows us to develop a thermomechanical theory in which higher gradients of the temperature may enter in the equilibrium set of the rate-dependent constitutive relation $(8)_1$. Such a non-local model will be presented elsewhere and it is in agreement with thermomechanical theories like that proposed by Maxwell (1879) in which the stress explicitly depends on spatial gradients of temperature.

3.1 A local Maxwell rate-type model

We consider in the following some simplified constitutive assumptions which are justified by experimental and theoretical results on the thermomechanical behavior of shape memory alloys.

It is known that thermoelasticity theories with non-monotone stress-strain relation for certain ranges of temperature is a main ingredient to describe solid-solid phase transitions in tensile bars (see Ericksen, 1975; Abeyaratne and Knowles, 1994 and the literature therein). On the other hand, starting from the good results obtained in modelling transformation pseudo-elasticity in the isothermal case by using a Maxwellian viscoelastic approach to non-monotone elasticity (see for instance Făciu and Suliciu, 1994), we have extended it (see Făciu and Mihăilescu-Suliciu, 2002a) in order to include thermal effects which accompany phase transition phenomena.

We first suppose that the constitutive function G (i.e. the equilibrium set $\mathcal{E}$) does not depend on θ_X and

$$G(\varepsilon, \sigma, \theta) = 0 \quad \text{if and only if} \quad \sigma = \sigma_R(\varepsilon, \theta), \tag{12}$$

where $\sigma_R : \mathcal{P} \subset (-1, \infty) \times R^+ \to R$, is called the *thermoelastic equilibrium surface* and it is a continuous and piecewise smooth function on $\mathcal{P}$, where $\mathcal{P}$ is the projection of $\mathcal{D}$ on the (ε, θ) plane.

A second assumption is

$$(\sigma - \sigma_R(\varepsilon, \theta))G(\varepsilon, \sigma, \theta) \leq 0, \quad \text{for any} \quad (\varepsilon, \sigma, \theta) \in \mathcal{D}. \tag{13}$$

It represents the necessary and sufficient condition that the equilibrium surface $\sigma = \sigma_R(\varepsilon, \theta)$ of a viscoelastic material be stable from above (respectively below) with respect to non-constant stress processes starting above (respectively below) the equilibrium surface. That is, each process starting at a given initial strain-stress-temperature state $(\varepsilon_0(X), \sigma_0(X), \theta_0(X)) \in \mathcal{D}$ such that $\sigma_0(X) > \sigma_R(\varepsilon_0(X), \theta_0(X))$ (respectively $\sigma_0(X) < \sigma_R(\varepsilon_0(X), \theta_0(X))$) move in the direction of decreasing (respectively increasing) stress. This assumption reflects some experimental evidence.

Concerning the axial heat flux q we adopt the usual constitutive relation, i.e. the Fourier law

$$\hat{q}(\varepsilon, \sigma, \theta, \theta_X) = -\kappa(\varepsilon, \sigma, \theta,)\frac{\partial \theta}{\partial X} \tag{14}$$

where $\kappa = \kappa(\varepsilon, \sigma, \theta,)$, $\kappa : \mathcal{D} \to R$ is the heat conduction coefficient.

By using assumptions (12), (13) and (14) into the dissipation inequality (11) we get the following two restrictions

$$\varrho \frac{\partial \hat{\psi}}{\partial \sigma}(\varepsilon, \sigma, \theta) G(\varepsilon, \sigma, \theta) \leq 0, \quad \text{for any } (\varepsilon, \sigma, \theta) \in \mathcal{D} \tag{15}$$

and

$$\kappa = \kappa(\varepsilon, \sigma, \theta) \geq 0 \qquad \text{for any } (\varepsilon, \sigma, \theta) \in \mathcal{D}, \tag{16}$$

which express the fact that in this case both internal dissipation and thermal dissipation have to be positive.

The constitutive relations (8) may now be written as

$$\begin{aligned}
&\frac{\partial \sigma}{\partial t} = E \frac{\partial \varepsilon}{\partial t} + G(\varepsilon, \sigma, \theta), \\
&e = \hat{e}(\varepsilon, \sigma, \theta) = \left(\psi - \theta \frac{\partial \psi}{\partial \theta} \right)(\varepsilon, \sigma, \theta), \qquad \frac{\partial^2 \hat{\psi}}{\partial \theta^2} \neq 0 \\
&\psi = \hat{\psi}(\varepsilon, \sigma, \theta), \\
&q = \hat{q}(\varepsilon, \sigma, \theta) = -\kappa(\varepsilon, \sigma, \theta) \theta_X, \qquad \kappa > 0,
\end{aligned} \tag{17}$$

where the free energy function $\psi = \hat{\psi}(\varepsilon, \sigma, \theta)$, if it exists, have to verify the following two relations

$$\frac{\partial \hat{\psi}}{\partial \varepsilon} + E \frac{\partial \hat{\psi}}{\partial \sigma} = \frac{\sigma}{\varrho}, \quad \varrho \frac{\partial \hat{\psi}}{\partial \sigma} G(\varepsilon, \sigma, \theta) \leq 0, \qquad \text{for any } (\varepsilon, \sigma, \theta) \in \mathcal{D} \tag{18}$$

In the next section we deduce the additional constitutive restrictions on the thermoelastic equilibrium surface $\sigma = \sigma_R(\varepsilon, \sigma)$ that ensure the existence of a unique free energy function for our Maxwellian thermo-viscoelastic approach and we construct it.

Let us note that the simplest example of a relaxation function G is given by

$$G(\varepsilon, \sigma, \theta) = -k(\sigma - \sigma_R(\varepsilon, \theta)), \qquad (\varepsilon, \sigma, \theta) \in \mathcal{D} \tag{19}$$

where k is constant, and positive according to (15); k is called the Maxwellian viscosity coefficient ($1/k$ is a relaxation time of the material).

It is useful to note that the balance of energy equation $(5)_3$ can be written now only by means of the free energy function and the complete PDEqs system for the unknown functions v, ε, σ, θ describing the thermo-mechanical motion of the viscoelastic bar becomes

$$
\begin{aligned}
&\varrho\frac{\partial v}{\partial t} - \frac{\partial \sigma}{\partial X} = \frac{2R'(X)}{R(X)}\sigma + \varrho b,\\
&\frac{\partial \varepsilon}{\partial t} - \frac{\partial v}{\partial X} = 0,\\
&\frac{\partial \sigma}{\partial t} - E\frac{\partial \varepsilon}{\partial t} = G(\varepsilon,\sigma,\theta),\\
&C\frac{\partial \theta}{\partial t} - \frac{\kappa}{\varrho}\frac{\partial^2 \theta}{\partial X^2} - \frac{\kappa}{\varrho}\frac{2R'(X)}{R(X)}\frac{\partial \theta}{\partial X} = -\frac{\partial \psi}{\partial \sigma}G + \theta\frac{\partial^2 \psi}{\partial \theta \partial \sigma}G - \frac{2\omega}{\varrho R(X)}(\theta - \theta_o) + r,
\end{aligned}
\tag{20}
$$

where

$$
C = C(\varepsilon,\theta,\sigma) \equiv -\theta\frac{\partial^2 \psi}{\partial \theta^2}(\varepsilon,\theta,\sigma) = \frac{\partial \hat{e}}{\partial \theta}(\varepsilon,\theta,\sigma). \tag{21}
$$

is called the non-equilibrium *heat capacity* of the material.

The heat propagation equation $(20)_4$ contains in the left-hand side the classical term describing thermal dissipation through axial conduction. Beside that, in the right-hand side we have a first term which describes the internal dissipation, a second one which is related with the latent heat released or absorbed by the material, while the third one gives account on the gain or loss of heat across the lateral surface of the bar. The terms which describe the influence of the geometrical defect are present in the balance of momentum and balance of energy and lead to stress and temperature concentrations as will be seen in the numerical experiments of Section 6.

3.2 The free energy of the thermo-viscoelastic model

In the isothermal case the existence of a free energy for rate-type semilinear viscoelastic constitutive equations with non-monotone stress-strain relation has been investigated in Făciu and Mihăilescu-Suliciu, (1987). In that approach we construct rather than postulate the free energy function starting from the constitutive information available for the equilibrium stress-strain relation. In this section we extend this result to the non-isothermal constitutive structure (17) verifying assumptions (12-13).

Suppose the equilibrium surface $\sigma = \sigma_R(\varepsilon,\theta)$ is continuous and piecewise smooth on $\mathcal{P} = I_\varepsilon \times I_\theta$, $I_\varepsilon = [\varepsilon_I, \varepsilon_{II}]$, $I_\theta = [\theta_I, \theta_{II}]$ and let us take

$$
\mathcal{D} \equiv \{(\varepsilon,\theta,\sigma_R(\tilde{\varepsilon},\theta) + E(\varepsilon - \tilde{\varepsilon})) \mid \varepsilon,\tilde{\varepsilon} \in I_\varepsilon, \theta \in I_\theta\}. \tag{22}
$$

Our main result is the following. The system (18) has a unique solution (up to an additive function of θ) $\psi = \hat{\psi}(\varepsilon, \theta, \sigma) : \mathcal{D} \longrightarrow R$ which is continuous, smooth with respect to (ε, σ) and piecewise smooth with respect to θ on $\mathcal{D}$ if and only if

$$\frac{\sigma_R(\varepsilon_1, \theta) - \sigma_R(\varepsilon_2, \theta)}{\varepsilon_1 - \varepsilon_2} < E \ \text{ for any } \ \varepsilon_1, \varepsilon_2 \in I_\varepsilon \ , \ \varepsilon_1 \neq \varepsilon_2 \ , \ \theta \in I_\theta. \tag{23}$$

This condition allows us to consider materials for which the equilibrium curve has not always a positive slope like those which are used to characterize phase transformations (see Abeyaratne and Knowles, 1994) and plastic flow material instabilities (see Molinari and Clifton, 1987).

Moreover, the free energy function has the form

$$\varrho \hat{\psi}(\varepsilon, \theta, \sigma) = \frac{\sigma^2}{2E} + \phi(\sigma - E\varepsilon, \theta) \tag{24}$$

with

$$\begin{aligned} \phi(\tau, \theta) - \phi(\tau_o, \theta) = -\frac{1}{2E}(\tau^2 - \tau_o^2) - \int_{\tau_o}^{\tau} \bar{h}(p, \theta) dp = \\ -\frac{1}{2E}\left(\sigma_R^2(\bar{h}(\tau, \theta), \theta) - \sigma_R^2(\bar{h}(\tau_o, \theta), \theta)\right) + \int_{\bar{h}(\tau_o, \theta)}^{\bar{h}(\tau, \theta)} \sigma_R(s, \theta) ds, \end{aligned} \tag{25}$$

and

$$\tau_o \in h(I_\varepsilon, \theta) \quad \text{for any} \quad \theta \in I_\theta. \tag{26}$$

In relations (25) and (26) we denote by

$$h(\varepsilon, \theta) \equiv \sigma_R(\varepsilon, \theta) - E\varepsilon, \quad h : I_\varepsilon \times I_\theta \longrightarrow R, \tag{27}$$

and by $\bar{h} = \bar{h}(\tau, \theta)$ its inverse with respect to ε for a fixed θ, that is

$$\begin{aligned} &\bar{h}(h(\varepsilon, \theta), \theta) \equiv \varepsilon, \text{for any } \varepsilon \in I_\varepsilon, \ \theta \in I_\theta, \\ &h(\bar{h}(\tau, \theta), \theta) \equiv \tau, \text{for any } \tau \in h(I_\varepsilon, \theta), \ \theta \in I_\theta. \end{aligned} \tag{28}$$

We also have, as a direct consequence of $(18)_2$, that

$$\frac{\partial \psi}{\partial \sigma}(\varepsilon, \theta, \sigma_R(\varepsilon, \theta)) = 0. \tag{29}$$

The equilibrium energy function and the equilibrium entropy

$$\begin{aligned} \varrho \psi_R(\varepsilon, \theta) \equiv& \varrho \hat{\psi}(\varepsilon, \theta, \sigma_R(\varepsilon, \theta)) \\ =& \frac{1}{2E}\sigma_R^2(\bar{h}(\tau_o, \theta), \theta) + \phi(\tau_o, \theta) + \int_{\bar{h}(\tau_o, \theta)}^{\varepsilon} \sigma_R(s, \theta) ds \\ \eta_R(\varepsilon, \theta) \equiv& \hat{\eta}(\varepsilon, \theta, \sigma_R(\varepsilon, \theta)) \end{aligned} \tag{30}$$

are exactly the thermo-elastic energy and entropy functions corresponding to the non-linear thermo-elastic constitutive relation $\sigma = \sigma_R(\varepsilon,\theta)$ since

$$\varrho\frac{\partial\psi_R}{\partial\varepsilon}(\varepsilon,\theta) = \sigma_R(\varepsilon,\theta)\ ,\ \frac{\partial\psi_R}{\partial\theta}(\varepsilon,\theta) = -\eta_R(\varepsilon,\theta). \tag{31}$$

For our thermo-viscoelastic model whenever the equilibrium free-energy function $\psi_R(\varepsilon,\theta)$ is non-convex with respect to strain on certain intervals of temperature the energy function $\varphi = \varphi(\sigma - E\varepsilon,\theta)$ is also non-convex with respect to $\sigma - E\varepsilon$ for the corresponding ranges of temperature (see Fig.4 and Fig.5) .

Remark 4. In order to obtain a continuous and piecewise smooth free energy function with respect to θ on $\mathcal{D}$ the function $\phi(\tau_o,\theta)$ has to be continuous and piecewise smooth as function of θ. The existence of a τ_o with property (26) is not a necessary condition as we may choose a different $\tau_o \in h(I_\varepsilon,\theta)$ for each $\theta \in I_\theta$, i.e. $\tau_o = \tau_o(\theta)$, but we shall find out in what follows that quite another type of condition ensures the existence of at least a τ_o with property (26).

Remark 5. The solution (24)+(25) of the system (18) may be constructed on the domain $\mathcal{D}$ only, which justifies why we have chosen this domain. All the constitutive functions need then to be defined on $\mathcal{D}$ only as we are not interested in states $(\varepsilon,\sigma,\theta)$ where no free energy can be defined. Yet there is another strong argument in choosing the domain $\mathcal{D}$. Indeed, by an appropriate choice of the domain $\mathcal{P}$ any process starting in the corresponding domain $\mathcal{D}$ remains in $\mathcal{D}$ as long as it lasts. This essential property is proved in the following result.

Let $\mathcal{P}$ have the form

$$\mathcal{P} = \{(\varepsilon,\theta) \mid \varepsilon \in I_\varepsilon(\theta) = [\varepsilon_I(\theta),\varepsilon_{II}(\theta)]\ ,\ \theta \in I_\theta = [\theta_I,\theta_{II}]\}, \tag{32}$$

i.e.

$$\mathcal{D} = \{(\varepsilon,\theta,\sigma = E\varepsilon + h(\tilde{\varepsilon},\theta)) \mid \varepsilon,\tilde{\varepsilon} \in I_\varepsilon(\theta)\ ,\ \theta \in I_\theta\}, \tag{33}$$

with $\varepsilon_I(\theta)$, $\varepsilon_{II}(\theta)$ continuous and piecewise smooth on I_θ and let $\sigma_R(\varepsilon,\theta)$ be defined, continuous and piecewise smooth on $\mathcal{P}$.

Then any homogeneous process $(\varepsilon(t),\theta(t),\sigma(t))$, $t \in [0,\bar{t})$ that starts in $\mathcal{D}$, i.e. $(\varepsilon(0),\theta(0),\sigma(0)) \in \mathcal{D}$ with the property that $\varepsilon(t) \in I_\varepsilon(\theta(t))$ for any $t \in [0,\bar{t})$ remains in $\mathcal{D}$ for any $t \in (0,\bar{t})$ iff there exist $h_I=$ const. , $h_{II}=$ const. such that

$$\varepsilon_I(\theta) = \bar{h}(h_I,\theta)\ ,\ \varepsilon_{II}(\theta) = \bar{h}(h_{II},\theta) \text{ for any } \theta \in I_\theta. \tag{34}$$

Moreover the above result does also show there are at least two values for τ_o with property (26).

Remark 6. It is worth noting that the free energy function does not depend on the expression of $G(\varepsilon, \theta, \sigma)$ and its properties except for condition (13). Thus, the same as for the isothermal case, the free energy function (24)+(25) will also be a free energy function for any thermo-viscoplastic rate-type material (8) for which the corresponding function $\tilde{G}(\varepsilon, \theta, \sigma)$ is such that the equilibrium surface of our thermo-viscoelastic material is contained in the equilibrium set $\{(\varepsilon, \theta, \sigma); \tilde{G}(\varepsilon, \theta, \sigma) = 0\}$ of the thermo-viscoplastic material.

Remark 7. According to (25) the expression of the free energy contains a still undetermined function of temperature. But even in the thermo-elastic case a complete constitutive set requires either the knowledge of the free energy $\psi = \psi_R(\varepsilon, \theta)$ and then $\sigma = \sigma_R(\varepsilon, \theta)$ and $\eta = \eta_R(\varepsilon, \theta)$ result from (31), or the knowledge of $\sigma = \sigma_R(\varepsilon, \theta)$ and $\eta = \eta_R(\varepsilon, \theta)$ and then $\psi = \psi_R(\varepsilon, \theta)$ is completely determined from (31). In our case the situation is the same. In order to construct $\psi_R(\varepsilon, \theta)$ we need also to know, beside the function $\sigma_R(\varepsilon, \theta)$, the function $\eta_R(\varepsilon, \theta)$ along a non-isothermal curve in $\mathcal{P}$. Then, with a complete knowledge of the equilibrium properties and the way they extend outside equilibrium (by means of the dynamic Young modulus E), the expression of $\hat{\psi}(\varepsilon, \theta, \sigma)$ is completely determined as one may see from (25) and (26). An additional constitutive assumption is therefore needed and it usually concerns the heat capacity $C(\varepsilon, \theta, \sigma)$ defined in (21). According to assumption $(8)_2$, C has to be strictly different from zero while, on the other hand, experimental evidence shows it is always positive. Thus the constitutive information should be completed with a given strictly positive function for the heat capacity C.

4 Related materials with one internal variable

The constitutive set (8) is equivalent to that for a material with one internal variable α

$$
\begin{aligned}
\sigma &= \tilde{\sigma}(\varepsilon, \theta, \theta_X, \alpha) \\
e &= \tilde{e}(\varepsilon, \theta, \theta_X, \alpha) \\
\psi &= \tilde{\psi}(\varepsilon, \theta, \theta_X, \alpha) \\
q &= \tilde{q}(\varepsilon, \theta, \theta_X, \alpha) \\
\frac{\partial \alpha}{\partial t} &= \bar{f}(\varepsilon, \theta, \theta_X, \alpha),
\end{aligned}
\tag{35}
$$

which has the property

$$\frac{\partial \tilde{\sigma}}{\partial \theta} \equiv 0 \text{ and } \frac{\partial \tilde{\sigma}}{\partial \alpha} \neq 0 \quad \text{for any } (\varepsilon, \theta, \theta_X, \alpha) \in \Omega. \tag{36}$$

In (35) and (36) the functions $(\tilde{\sigma}, \tilde{e}, \tilde{\psi}, \tilde{q}, \bar{f})$ are considered continuous and piecewise smooth on a domain $\Omega \subset (-1, \infty) \times R^{+} \times R \times R$. Indeed, let us recall first from the theory of materials with internal state variables that the constitutive set (35+36) is compatible with the second law of thermodynamics (6) iff it has the form

$$\begin{aligned}
&\sigma = \tilde{\sigma}(\varepsilon, \theta, \alpha) = \varrho \frac{\partial \tilde{\psi}}{\partial \varepsilon}(\varepsilon, \theta, \alpha) \\
&e = \tilde{e}(\varepsilon, \theta, \alpha) = \left(\tilde{\psi} - \theta \frac{\partial \tilde{\psi}}{\partial \theta} \right)(\varepsilon, \theta, \alpha) \\
&\psi = \tilde{\psi}(\varepsilon, \theta, \alpha) \\
&\eta = -\frac{\partial \tilde{\psi}}{\partial \theta}(\varepsilon, \theta, \alpha) \\
&q = \tilde{q}(\varepsilon, \theta, \theta_X, \alpha) \\
&\frac{\partial \alpha}{\partial t} = \bar{f}(\varepsilon, \theta, \theta_X, \alpha),
\end{aligned} \tag{37}$$

and

$$\frac{\partial \tilde{\sigma}}{\partial \theta} \equiv 0 \ , \ \frac{\partial \tilde{\sigma}}{\partial \alpha} \neq 0 \ , \ \frac{\partial \tilde{\psi}}{\partial \alpha} \bar{f} + \frac{1}{\varrho \theta} q \theta_X \leq 0 \quad \text{for any } (\varepsilon, \theta, \alpha) \in \bar{\Omega}, \tag{38}$$

where $\bar{\Omega}$ is the projection of Ω on the $(\varepsilon, \theta, \alpha)$-space. Now, if we consider the set (37+38), conditions $(38)_{1,2}$ allow relation $(37)_1$ to be inverted with respect to α under the form

$$\alpha = \tilde{\alpha}(\varepsilon, \sigma) \ , \ \tilde{\sigma}(\varepsilon, \tilde{\alpha}(\varepsilon, \sigma)) \equiv \sigma, \tag{39}$$

while the time derivative of $(37)_1$ gives

$$\frac{\partial \sigma}{\partial t} = \frac{\partial \tilde{\sigma}}{\partial \varepsilon}(\varepsilon, \tilde{\alpha}(\varepsilon, \sigma)) \frac{\partial \varepsilon}{\partial t} + \frac{\partial \tilde{\sigma}}{\partial \alpha}(\varepsilon, \tilde{\alpha}(\varepsilon, \sigma)) \bar{f}(\varepsilon, \theta, \theta_X, \tilde{\alpha}(\varepsilon, \sigma)). \tag{40}$$

With the notations

$$\begin{aligned}
E(\varepsilon, \sigma) &\equiv \frac{\partial \tilde{\sigma}}{\partial \varepsilon}(\varepsilon, \tilde{\alpha}(\varepsilon, \sigma)) \\
G(\varepsilon, \theta, \sigma, \theta_X) &\equiv \frac{\partial \tilde{\sigma}}{\partial \alpha}(\varepsilon, \tilde{\alpha}(\varepsilon, \sigma)) \bar{f}(\varepsilon, \theta, \theta_X, \tilde{\alpha}(\varepsilon, \sigma)),
\end{aligned} \tag{41}$$

relation (40) becomes $(8)_1$, relations $(37)_{2-5}$ become $(8)_{2-5}$ with the restrictions $(10)_{1,3}$, relation $(37)_1$ turns into $(10)_2$ while inequality $(38)_3$ turns into (11). Condition $(38)_1$ makes sure there is no term containing the rate of temperature in (40) respectively $(8)_1$.

Now let us consider a rate-type constitutive set (8) satisfying (10+11) with the notation $\alpha \equiv \sigma - E\varepsilon$. Then equation $(8)_1$ may be written as

$$\frac{\partial \alpha}{\partial t} = G(\varepsilon, \theta, \sigma = \alpha + E\varepsilon, \theta_X) = \tilde{G}(\varepsilon, \theta, \alpha, \theta_X),$$

and the constitutive set (8+10+11) may then obviously be written under the form (37+38).

Remark 8. Let us also note that I.Suliciu in Cristescu and Suliciu, (1982) proved the equivalence between constitutive relations with internal state variables and rate-type constitutive relations in stress, entropy, free energy and heat flux possessing instantaneous response (in stress, entropy, free energy and heat flux) at any state.

5 The equilibrium stress-strain-temperature surface: an example

The equilibrium stress-strain-temperature constitutive relation $\sigma = \sigma_R(\varepsilon, \theta)$ plays a key role in our constitutive set for a thermo-viscoelastic rate-type material as, according to the previous sections, it determines the form of the equilibrium free energy function (up to a function of temperature).

In this section we construct an explicit (and rather simple) stress-strain-temperature relation that characterizes the response of a three-phase SMA and prove that the corresponding constitutive set may describe the main properties of this material as found out in laboratory tests. The thermo-elastic equilibrium surface we consider here is similar to that derived from physical considerations on the behavior of shape memory alloys by Abeyaratne et al. (1994) .

We consider a material which exists in a high-temperature austenite (A) phase and has two variants (M^- and M^+) of a low-temperature martensite phase. The thermomechanical assumptions we consider here are the following. There are two critical temperatures θ_m and θ_M such as, for $\theta > \theta_M$ the material only exists in its austenite form no matter what the stress level is, whereas for $\theta < \theta_m$ the material only exists in its martensitic forms. For $\theta \in [\theta_m, \theta_M]$ all three phases are available to the material.

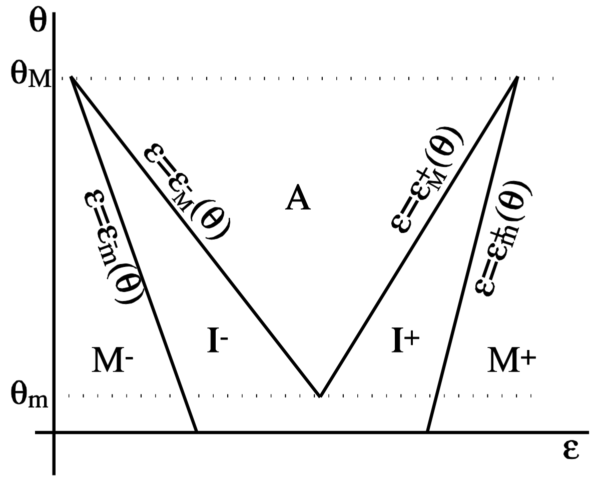

Figure 2: Austenite (A), martensite ($M^{\pm}$) and unstable ($I^{\pm}$) regions in the (ε, θ)-plane.

Thus: a) the stress response function σ_R is a monotonically increasing function of strain for $\theta > \theta_M$; b) at each temperature $\theta \in [\theta_m, \theta_M]$ the equilibrium response function $\sigma_R(\varepsilon, \theta)$ is a monotonically increasing function of strain for $\varepsilon \in (\varepsilon_I(\theta), \varepsilon_m^-(\theta)) \cup (\varepsilon_M^-(\theta), \varepsilon_M^+(\theta)) \cup (\varepsilon_m^+(\theta), \varepsilon_{II}(\theta))$ and a monotonically decreasing function of strain over the intervals $(\varepsilon_m^-(\theta), \varepsilon_M^-(\theta))$ and $(\varepsilon_M^+(\theta), \varepsilon_m^+(\theta))$; c) for $\theta < \theta_m$, $\sigma_R(\varepsilon, \theta)$ is a monotonically increasing function of strain on two intervals, i.e. $(\varepsilon_I(\theta), \varepsilon_m^-(\theta)) \cup (\varepsilon_m^+(\theta), \varepsilon_{II}(\theta))$ while on the remaining one $(\varepsilon_m^-(\theta), \varepsilon_m^+(\theta))$ it is monotonically decreasing.

Experiments on shape memory alloys (see for instance Otsuka et al., 1976) show that a material in a single phase has in general a linear thermoelastic behavior. Then we may assume that the elastic moduli of the austenite phase A and martensite variants $M^{\pm}$ are constant and equal to $E_1 > 0$ and $E_3 > 0$, respectively. Moreover, we suppose here that the elastic moduli of the unstable (spinodal) regions $I^{\pm}$ are also constant and equal to $-E_2 < 0$.

We therefore write

$$\sigma_R : \mathcal{P} \subset R^2 \longrightarrow R \ , \ \mathcal{P} = \{(\varepsilon, \theta); \varepsilon \in (\varepsilon_I(\theta), \varepsilon_{II}(\theta)), \theta \in (\theta_I, \theta_{II}) \supset [\theta_m, \theta_M]\}$$

where , according to one of the above remarks ,

$$\sigma_R(\varepsilon_I(\theta), \theta) - E\varepsilon_I(\theta) = h_I = \text{const.}$$
$$\sigma_R(\varepsilon_{II}(\theta), \theta) - E\varepsilon_{II}(\theta) = h_{II} = \text{const.}$$

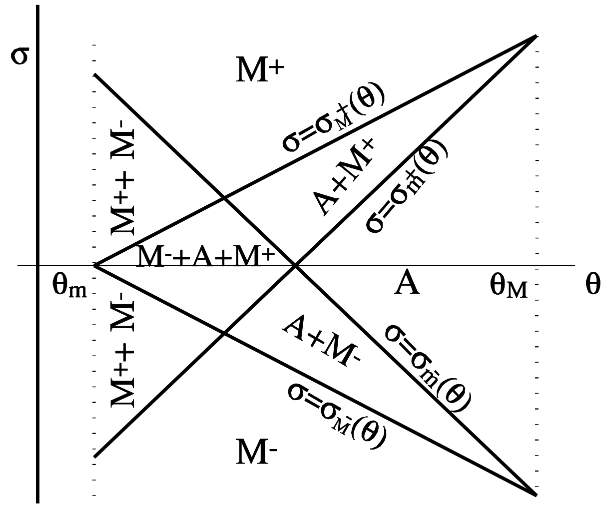

Figure 3: Available phases at a given (σ, θ).

for any $\theta \in [\theta_I, \theta_{II}]$. The expression of $\sigma_R(\varepsilon, \theta)$ for $\theta \in [\theta_m, \theta_M]$ is taken as

$$\sigma_R(\varepsilon, \theta) = \begin{cases} E_3(\varepsilon - \varepsilon_m^-(\theta)) + \sigma_m^-(\theta), & \text{if } \varepsilon_I(\theta) \leq \varepsilon \leq \varepsilon_m^-(\theta) \\ -E_2(\varepsilon - \varepsilon_m^-(\theta)) + \sigma_m^-(\theta) & \text{if } \varepsilon_m^-(\theta) < \varepsilon < \varepsilon_M^-(\theta) \\ E_1(\varepsilon - \varepsilon_M^-(\theta)) + \sigma_M^-(\theta) & \text{if } \varepsilon_M^-(\theta) \leq \varepsilon \leq \varepsilon_M^+(\theta) \\ -E_2(\varepsilon - \varepsilon_M^+(\theta)) + \sigma_M^+(\theta) & \text{if } \varepsilon_M^+(\theta) < \varepsilon < \varepsilon_m^+(\theta) \\ E_3(\varepsilon - \varepsilon_m^+(\theta)) + \sigma_m^+(\theta) & \text{if } \varepsilon_m^+(\theta) \leq \varepsilon < \varepsilon_{II}(\theta), \end{cases} \tag{42}$$

with

$$0 < E_1 = \text{const.} < E, \qquad 0 < E_3 = \text{const.} < E. \tag{43}$$

Here the functions $\sigma_M^\pm(\theta) = \sigma_R(\varepsilon_M^\pm(\theta), \theta)$ and $\sigma_m^\pm(\theta) = \sigma_R(\varepsilon_m^\pm(\theta), \theta)$ are the local maxima and minima with respect to ε of the stress-strain curve at constant temperature. In our approach we call $\sigma = \sigma_M^\pm(\theta)$ ($\varepsilon = \varepsilon_M^\pm(\theta)$) the stress (strain) required for the $A \to M^\pm$ transformations, whereas $\sigma = \sigma_m^\pm(\theta)$ ($\varepsilon = \varepsilon_m^\pm(\theta)$) the stress (strain) required for the reverse $M^\pm \to A$ transformations when $\theta \in [\theta_I, \theta_{II}]$.

The boundary curves $\varepsilon = \varepsilon_I(\theta), \varepsilon = \varepsilon_{II}(\theta), \varepsilon = \varepsilon_m^\pm(\theta)$ and $\varepsilon = \varepsilon_M^\pm(\theta)$ fix the limits of the regions of the (ε, θ)-plane on which the respective phases A, M^+ and M^- exist (see for instance Fig.2).

Due to the symmetry of the two variants of martensite we require

$$\sigma_M^-(\theta) = -\sigma_M^+(\theta) \quad \text{and} \quad \sigma_m^-(\theta) = -\sigma_m^+(\theta), \quad \text{for any} \quad \theta \in [\theta_m, \theta_M], \tag{44}$$

while, due to the continuity of the equilibrium surface, we have

$$
\begin{aligned}
\sigma_M^-(\theta) &= -E_2(\varepsilon_M^-(\theta) - \varepsilon_m^-(\theta)) + \sigma_m^-(\theta) \\
\sigma_M^+(\theta) &= E_1(\varepsilon_M^+(\theta) - \varepsilon_M^-(\theta)) + \sigma_M^-(\theta) \\
\sigma_m^+(\theta) &= -E_2(\varepsilon_m^+(\theta) - \varepsilon_M^-(\theta)) + \sigma_M^+(\theta).
\end{aligned}
\tag{45}
$$

From (44) and (45) we get then

$$
\begin{aligned}
\sigma_M^+(\theta) &= \frac{E_1}{2}(\varepsilon_M^+(\theta) - \varepsilon_M^-(\theta)) \\
\sigma_m^+(\theta) &= E_2(\varepsilon_m^-(\theta) - \varepsilon_M^-(\theta)) + \frac{E_1}{2}(\varepsilon_M^+(\theta) - \varepsilon_M^-(\theta))
\end{aligned}
\tag{46}
$$

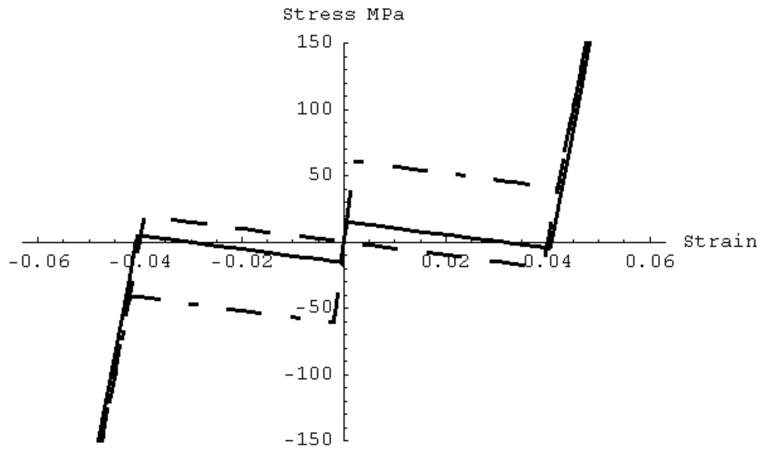

Figure 4: Stress-strain curves at constant temperature θ described by relations (58-60) for the numerical entries (90); 270^0K - dashed line, 285^0K - solid line, 300^0K - dot-dashed line.

The equilibrium stress-strain-temperature relation (42) is intended to describe a piecewise linear thermoelastic behavior thus we require the functions $\varepsilon = \varepsilon_m^\pm(\theta)$ and $\varepsilon = \varepsilon_M^\pm(\theta)$ to be linear in θ as well as the functions $\sigma = \sigma_m^\pm(\theta)$ and $\sigma = \sigma_M^\pm(\theta)$; moreover, according to our previous thermomechanical assumptions (see Figs.2,3), they have to satisfy the conditions

$$
\begin{aligned}
&\sigma_M^+(\theta_M) = \sigma_m^+(\theta_M), \quad \varepsilon_M^+(\theta_M) = \varepsilon_m^+(\theta_M), \quad \varepsilon_M^-(\theta_M) = \varepsilon_m^-(\theta_M), \\
&\sigma_M^+(\theta_m) = 0, \quad \varepsilon_M^+(\theta_m) = \varepsilon_M^-(\theta_m),
\end{aligned}
\tag{47}
$$

By assuming that the undeformed material in the A phase is stress free at a reference temperature $\theta_T \in (\theta_m, \theta_M)$, i.e., $\sigma_R(0, \theta_T) = 0$ we get from (42), (46)

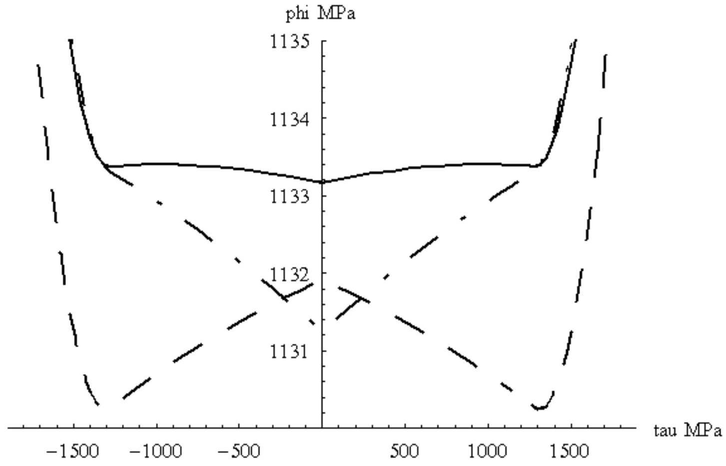

Figure 5: The energy function $\phi = \phi(\sigma - E\varepsilon, \theta)$ at constant temperatures corresponding to stress-strain relations (58-60) and numerical entries (90); $270^0 K$ - dashed line, $285^0 K$ - solid line, $300^0 K$ - dot-dashed line.

and (47)

$$
\begin{aligned}
\varepsilon_M^+(\theta) &= \alpha(\theta - \theta_T) + M(\theta - \theta_m) \\
\varepsilon_m^+(\theta) &= \alpha(\theta - \theta_T) - (M - m)(\theta - \theta_M) + M(\theta - \theta_m) \\
\varepsilon_M^-(\theta) &= \alpha(\theta - \theta_T) - M(\theta - \theta_m) \\
\varepsilon_m^-(\theta) &= \alpha(\theta - \theta_T) + (M - m)(\theta - \theta_M) - M(\theta - \theta_m)
\end{aligned}
\tag{48}
$$

and

$$
\begin{aligned}
\sigma_M^+(\theta) &= -\sigma_M^-(\theta) = E_1 M(\theta - \theta_m) \\
\sigma_m^+(\theta) &= -\sigma_m^-(\theta) = E_2(M - m)(\theta - \theta_M) + E_1 M(\theta - \theta_m).
\end{aligned}
\tag{49}
$$

where α=const.¿0 is the thermal expansion coefficient of the material in phase A and M=const., m=const. are other two material constants.

Since the boundaries of the (A), (M^+) and (M^-) regions in the (ε, θ)-plane have to satisfy the inequalities

$$
-1 < \varepsilon_I(\theta) \leq \varepsilon_m^-(\theta) \leq \varepsilon_M^-(\theta) \leq \varepsilon_M^+(\theta) \leq \varepsilon_m^+(\theta) \leq \varepsilon_{II}(\theta), \text{ for any } \theta \in (\theta_m, \theta_M),
\tag{50}
$$

we derive the following restrictions on the material parameters entering (48) and (49): $M > 0 \qquad m < M$,. We therefore assume

$$
0 < \alpha < m < M,
\tag{51}
$$

while the first two inequalities as well as the last inequality in (50) are conditions to be verified for h_I and h_{II}.

Let us specify the meaning of the two constants m and M. It is known that one may determine the effect of temperature on nucleation stress (see for instance Shaw & Kyriakides, (1997)) by laboratory tests. Since according to relations (49), $E_1 M$ and $E_1 M + E_2(M - m)$ describe the rate at which the stresses required for the $A \to M^+$ and $M^+ \to A$ transformations respectively, vary with respect to temperature, the two constants m and M may therefore be determined when the elastic moduli E_i, $i = 1, 2, 3$ are already precised.

The equilibrium surface (42) may be extended continuously on (θ_I, θ_m) and (θ_M, θ_{II}) in different ways according to the above constitutive assumptions (and using the same pattern as in (42)). For example, we can now define the functions $\varepsilon_M^{\pm}(\theta)$ and $\varepsilon_m^{\pm}(\theta)$ in a continuous manner outside the interval (θ_m, θ_M) in the following way

$$\varepsilon_M^{+}(\theta) = \begin{cases} \alpha(\theta - \theta_T), & \text{if } \theta \in (\theta_I, \theta_m] \\ \alpha(\theta - \theta_T) + M(\theta - \theta_m), & \text{if } \theta \in (\theta_m, \theta_{II}) \end{cases} \tag{52}$$

$$\varepsilon_M^{-}(\theta) = \begin{cases} \alpha(\theta - \theta_T), & \text{if } \theta \in (\theta_I, \theta_m] \\ \alpha(\theta - \theta_T) - M(\theta - \theta_m), & \text{if } \theta \in (\theta_m, \theta_{II}) \end{cases} \tag{53}$$

$$\varepsilon_m^{+}(\theta) = \begin{cases} \alpha(\theta - \theta_T) - (M - m)(\theta - \theta_M) + M(\theta - \theta_m), & \text{if } \theta \in (\theta_I, \theta_M] \\ \alpha(\theta - \theta_T) + M(\theta - \theta_m), & \text{if } \theta \in (\theta_M, \theta_{II}) \end{cases} \tag{54}$$

$$\varepsilon_m^{-}(\theta) = \begin{cases} \alpha(\theta - \theta_T) + (M - m)(\theta - \theta_M) - M(\theta - \theta_m), & \text{if } \theta \in (\theta_I, \theta_M] \\ \alpha(\theta - \theta_T) - M(\theta - \theta_m), & \text{if } \theta \in (\theta_M, \theta_{II}) \end{cases} . \tag{55}$$

The functions $\sigma_M^{\pm}(\theta)$ and $\sigma_m^{\pm}(\theta)$ are determined according to relations (49) and the continuity of $\sigma_R(\varepsilon, \theta)$ and we obtain

$$\sigma_M^{+}(\theta) = -\sigma_M^{-}(\theta) = \begin{cases} 0, & \text{if } \theta \in (\theta_I, \theta_m] \\ E_1 M(\theta - \theta_m), & \text{if } \theta \in (\theta_m, \theta_{II}) \end{cases} \tag{56}$$

$$\sigma_m^{+}(\theta) = -\sigma_m^{-}(\theta) = \begin{cases} E_2(-M(\theta - \theta_m) + (M - m)(\theta - \theta_M)), & \text{if } \theta \in (\theta_I, \theta_m] \\ E_1 M(\theta - \theta_m) + E_2(M - m)(\theta - \theta_M), & \text{if } \theta \in (\theta_m, \theta_M) \\ E_1 M(\theta - \theta_m), & \text{if } \theta \in (\theta_M, \theta_{II}) \end{cases} . \tag{57}$$

It is now easy to see that by using the above definitions (52)-(57) of the functions $\varepsilon_m^{\pm}(\theta)$, $\varepsilon_M^{\pm}(\theta)$, $\sigma_m^{\pm}(\theta)$ and $\sigma_M^{\pm}(\theta)$ the equilibrium stress-strain-temperature relation (42) can be still used for $\theta \in (\theta_I, \theta_m) \cup (\theta_M, \theta_{II})$.

For a better understanding and comparison with the equilibrium surface considered by Abeyaratne et al. (1994) we give bellow the explicit expression of $\sigma_R(\varepsilon, \theta)$ for $\theta \in [\theta_I, \theta_{II}]$ (see also Fig. 2)

a) For $\theta \in [\theta_m, \theta_M]$

$$\sigma_R(\varepsilon,\theta) = \begin{cases} E_3\varepsilon - \alpha E_3(\theta-\theta_T) - (E_1-E_3)M(\theta-\theta_m) \\ -(E_2+E_3)(M-m)(\theta-\theta_M), \\ \qquad\qquad\qquad\qquad \text{if } \ \varepsilon \in [\varepsilon_I(\theta), \varepsilon_m^-(\theta) \\ -E_2\varepsilon + \alpha E_2(\theta-\theta_T) - (E_1+E_2)M(\theta-\theta_m), \\ \qquad\qquad\qquad\qquad \text{if } \ \varepsilon \in [\varepsilon_m^-(\theta), \varepsilon_M^-(\theta)) \\ E_1\varepsilon - \alpha E_1(\theta-\theta_T), \\ \qquad\qquad\qquad\qquad \text{if } \ \varepsilon \in [\varepsilon_M^-(\theta), \varepsilon_M^+(\theta)] \\ -E_2\varepsilon + \alpha E_2(\theta-\theta_T) + (E_1+E_2)M(\theta-\theta_m), \\ \qquad\qquad\qquad\qquad \text{if } \ \varepsilon \in (\varepsilon_M^+(\theta), \varepsilon_m^+(\theta)] \\ E_3\varepsilon - \alpha E_3(\theta-\theta_T) + (E_1-E_3)M(\theta-\theta_m) \\ +(E_2+E_3)(M-m)(\theta-\theta_M), \\ \qquad\qquad\qquad\qquad \text{if } \ \varepsilon \in (\varepsilon_m^+(\theta), \varepsilon_{II}(\theta)]. \end{cases} \tag{58}$$

b) For $\theta \in [\theta_I, \theta_m)$

$$\sigma_R(\varepsilon,\theta) = \begin{cases} E_3\varepsilon - \alpha E_3(\theta-\theta_T) + (E_2+E_3)[M(\theta-\theta_m) - (M-m)(\theta-\theta_M)] \\ \qquad\qquad\qquad\qquad \text{if } \ \varepsilon \in [\varepsilon_I(\theta), \varepsilon_m^-(\theta) \\ -E_2\varepsilon + \alpha E_2(\theta-\theta_T), \\ \qquad\qquad\qquad\qquad \text{if } \ \varepsilon \in [\varepsilon_m^-(\theta), \varepsilon_m^+(\theta)) \\ E_3\varepsilon - \alpha E_3(\theta-\theta_T) + (E_2+E_3)[-M(\theta-\theta_m) + (M-m)(\theta-\theta_M)] \\ \qquad\qquad\qquad\qquad \text{if } \ \varepsilon \in (\varepsilon_m^+(\theta), \varepsilon_{II}(\theta)]. \end{cases} \tag{59}$$

c) For $\theta \in [\theta_M, \theta_{II}]$

$$\sigma_R(\varepsilon,\theta) = \begin{cases} E_3\varepsilon - \alpha E_3(\theta-\theta_T) - (E_1-E_3)M(\theta-\theta_m) \\ \qquad\qquad\qquad\qquad \text{if } \ \varepsilon \in [\varepsilon_I(\theta), \varepsilon_M^-(\theta) \\ E_1\varepsilon - \alpha E_1(\theta-\theta_T), \\ \qquad\qquad\qquad\qquad \text{if } \ \varepsilon \in [\varepsilon_M^-(\theta), \varepsilon_M^+(\theta)] \\ E_3\varepsilon - \alpha E_3(\theta-\theta_T) + (E_1-E_3)M(\theta-\theta_m) \\ \qquad\qquad\qquad\qquad \text{if } \ \varepsilon \in (\varepsilon_M^+(\theta), \varepsilon_{II}(\theta)]. \end{cases} \tag{60}$$

In our approach we have considered different elastic moduli for the (A) phase and martensitic variants $(M^{\pm})$, but the main difference between our stress-strain-temperature relation and that considered by Abeyaratne et al. (1994) concerns the dependence on θ of the local minima/maxima of the stress-strain curve in $(M^+)/(M^-)$ phases. Thus, in the paper mentioned above $\sigma_m^+(\theta) = E_1M(\theta-\theta_m) - E_1(M-m)(\theta-\theta_M) - E_1\gamma_T$, where γ_T=const.> 0 is called the transformation strain. Consequently, the slope $-E_2$ of the straight line connecting $(\varepsilon_M^+(\theta), \sigma_M^+(\theta))$ and $(\varepsilon_m^+(\theta), \sigma_m^+(\theta))$ is temperature dependent, i.e., $E_2(\theta) = E_1[1 - \gamma_T/((M-m)(\theta - \theta_M))]$, and it becomes unbounded when $\theta \to \theta_M$ turning therefore σ_R into a discontinuous function.

Our approach has the advantage that it allows to extend in a continuous manner outside the interval (θ_m, θ_M) the functions $\varepsilon_M^\pm(\theta)$, $\varepsilon_m^\pm(\theta)$ and $\sigma_M^\pm(\theta)$, $\sigma_m^\pm(\theta)$ and thus to capture in a single linear description of the type (42) the thermo-mechanical considerations described at the beginning of this section for the entire range of temperature $[\theta_I, \theta_{II}] \supset [\theta_m, \theta_M]$.

Now by using relation (25) we can explicitly determine, modulo a function $\phi(\theta)$, the free energy function for our thermo-viscoelastic model when its equilibrium stress-strain-temperature relation is described by (58+60). The complete expressions of the free energy function $\psi(\varepsilon, \theta, \sigma)$ of the viscoelastic model, of the equilibrium free energy function $\psi_R(\varepsilon, \theta)$ and of the equilibrium entropy function $\eta_R(\varepsilon, \theta)$ are given in the next section. These expressions were used through the heat propagation equation $(20)_4$ in the numerical computations presented in the last section.

5.1 Corresponding thermodynamic potentials

In order to determine the equilibrium free energy and entropy we need, as mentioned above, some additional constitutive assumptions. We introduce the equilibrium heat capacity (at constant strain) or specific heat at constant strain

$$C_R(\varepsilon, \theta) \equiv -\theta \frac{\partial^2 \psi_R}{\partial \theta^2}(\varepsilon, \theta) = \frac{\partial e_R}{\partial \theta}(\varepsilon, \theta), \tag{61}$$

and make the assumption that it is constant and equal to $C > 0$ in the austenitic region (A), i.e., for $\varepsilon \in (\varepsilon_M^-(\theta), \varepsilon_M^+(\theta))$, $\theta \in (\theta_m, \theta_{II})$ as well as for $\varepsilon = \alpha(\theta_m - \theta_T), \theta \in (\theta_I, \theta_m)$; we also assume that $\psi_R(\varepsilon_o, \theta)$ is smooth at $(\varepsilon_o, \theta_m)$. This hypothesis automatically implies that $\psi_R(\varepsilon, \theta)$ is of C^2 class with respect to θ in region (A) while we already know it is at least of C^1 class with respect to ε in region (A).

Let us recall that the equilibrium free energy is the solution of equation $(31)_1$, i.e.

$$\varrho \psi_R(\varepsilon, \theta) = \varrho \psi_R(\varepsilon_o, \theta) + \int_{\varepsilon_o}^{\varepsilon} \sigma_R(s, \theta) ds, \tag{62}$$

with the choice

$$\varepsilon_o \equiv \alpha(\theta_m - \theta_T) = \varepsilon_M^\pm(\theta_m) \in [\varepsilon_M^-(\theta, \varepsilon_M^+(\theta)] \text{ for any } \theta \in [\theta_m, \theta_{II}]. \tag{63}$$

We therefore have, according to (62), to solve the equation in (A)

$$\frac{\partial^2 \psi_R}{\partial \theta^2}(\varepsilon_o, \theta) = -\frac{C}{\theta} \tag{64}$$

which has the general solution

$$\psi_R(\varepsilon_o,\theta)=\psi_R(\varepsilon_o,\theta_T)+(\theta-\theta_T)\left(\frac{\partial\psi_R}{\partial\theta}(\varepsilon_o,\theta_T)+C\right)-C\theta\ \ln\frac{\theta}{\theta_T}, \qquad (65)$$

for $\theta\in(\theta_m,\theta_{II})$. In order to fix the constants let us take

$$\psi_R(\varepsilon_o,\theta_T)=C\theta_T+\frac{\alpha^2E_1}{2\varrho}(\theta_m-\theta_T)^2\ ,\ \frac{\partial\psi_R}{\partial\theta}(\varepsilon_o,\theta_T)=-\frac{\alpha^2E_1}{\varrho}(\theta_m-\theta_T), \quad (66)$$

therefore

$$\varrho\psi_R(\varepsilon_o,\theta)=\varrho C\theta\left(1-\ln\frac{\theta}{\theta_T}\right)-\frac{\alpha^2E_1}{2}(\theta_m-\theta_T)(2\theta-\theta_m-\theta_T), \qquad (67)$$

for $\theta\in(\theta_m,\theta_{II})$. Relation (67) enables us to compute $\psi_R(\varepsilon,\theta)$ for $\varepsilon\in[\varepsilon_I(\theta),\varepsilon_{II}(\theta)],\theta\in[\theta_m,\theta_{II}]$, according to (62),(58) and (60). Moreover, once we know $\psi_R(\varepsilon,\theta)$ we may calculate the free energy function from (24) by taking into account that

$$\phi(\tau,\theta)=\varrho\psi_R(\bar h(\tau,\theta),\theta)-\frac{1}{2E}\sigma_R^2(\bar h(\tau,\theta),\theta). \qquad (68)$$

After some long but simple calculations we get the equilibrium free energy as follows.

a) For $\theta\in[\theta_m,\theta_M]$

$$\varrho\psi_R(\varepsilon,\theta)=\varrho C\theta\left(1-\ ln\frac{\theta}{\theta_T}\right)+$$

$$+\begin{cases}\frac{E_3}{2}\varepsilon^2+\varepsilon\Sigma_M^-(\theta)+\chi_M^-(\theta) & \text{if } \varepsilon\in(\varepsilon_I(\theta),\varepsilon_m^-(\theta))\\ -\frac{E_2}{2}\varepsilon^2+\varepsilon\Sigma^-(\theta)+\chi^-(\theta) & \text{if } \varepsilon\in(\varepsilon_m^-(\theta),\varepsilon_M^-(\theta))\\ \frac{E_1}{2}\varepsilon^2+\varepsilon\Sigma_A(\theta) & \text{if } \varepsilon\in(\varepsilon_M^-(\theta),\varepsilon_M^+(\theta))\\ -\frac{E_2}{2}\varepsilon^2+\varepsilon\Sigma^+(\theta)+\chi^+(\theta) & \text{if } \varepsilon\in(\varepsilon_M^+(\theta),\varepsilon_m^+(\theta))\\ \frac{E_3}{2}\varepsilon^2+\varepsilon\Sigma_M^+(\theta)+\chi_M^+(\theta) & \text{if } \varepsilon\in(\varepsilon_m^+(\theta),\varepsilon_{II}(\theta))\end{cases}\ , \qquad (69)$$

where we used the notations

$$\begin{aligned}\Sigma_M^-(\theta)=&-\alpha E_3(\theta-\theta_T)-(E_1-E_3)M(\theta-\theta_m)-(E_2+E_3)(M-m)(\theta-\theta_M)\\ \Sigma^-(\theta)=&\alpha E_2(\theta-\theta_T)-(E_1+E_2)M(\theta-\theta_m)\\ \Sigma_A(\theta)=&-\alpha E_1(\theta-\theta_T)\\ \Sigma^+(\theta)=&\alpha E_2(\theta-\theta_T)(E_1+E_2)M(\theta-\theta_m)\\ \Sigma_M^+(\theta)=&-\alpha E_3(\theta-\theta_T)(E_1-E_3)M(\theta-\theta_m)+(E_2+E_3)(M-m)(\theta-\theta_M)\end{aligned} \qquad (70)$$

and

$$
\begin{aligned}
\chi_M^-(\theta) =& - \frac{E_1+E_2}{2}[M(\theta-\theta_m)-\alpha(\theta-\theta_T)]^2 \\
&+ \frac{E_2+E_3}{2}[M(\theta-\theta_m)+(m-M)(\theta-\theta_M)-\alpha(\theta-\theta_T)]^2 \\
\chi^-(\theta) =& - \frac{E_1+E_2}{2}[M(\theta-\theta_m)-\alpha(\theta-\theta_T)]^2 \\
\chi^+(\theta) =& - \frac{E_1+E_2}{2}[M(\theta-\theta_m)+\alpha(\theta-\theta_T)]^2 \\
\chi_M^+(\theta) =& - \frac{E_1+E_2}{2}[M(\theta-\theta_m)+\alpha(\theta-\theta_T)]^2 \\
&+ \frac{E_2+E_3}{2}[M(\theta-\theta_m)+(m-M)(\theta-\theta_M)+\alpha(\theta-\theta_T)]^2.
\end{aligned}
\tag{71}
$$

b) For $\theta \in (\theta_M, \theta_{II}]$

$$
\varrho\psi_R(\varepsilon,\theta) = \varrho C\theta\left(1 - \ ln\frac{\theta}{\theta_T}\right) +
$$

$$
+ \begin{cases} \frac{E_3}{2}\varepsilon^2 + \varepsilon\Sigma_M^-(\theta) + \chi_M^-(\theta) & \text{if } \varepsilon \in [\varepsilon_I(\theta), \varepsilon_M^-(\theta)) \\ \frac{E_1}{2}\varepsilon^2 + \varepsilon\Sigma_A(\theta) & \text{if } \varepsilon \in [\varepsilon_M^-(\theta), \varepsilon_M^+(\theta)] \\ \frac{E_3}{2}\varepsilon^2 + \varepsilon\Sigma_M^+(\theta) + \chi_M^+(\theta) & \text{if } \varepsilon \in (\varepsilon_M^+(\theta), \varepsilon_{II}(\theta)] \end{cases}, \tag{72}
$$

with

$$
\begin{aligned}
\Sigma_M^-(\theta) =& - \alpha E_3(\theta-\theta_T) - (E_1-E_3)M(\theta-\theta_m) \\
\Sigma_A(\theta) =& - \alpha E_1(\theta-\theta_T) \\
\Sigma_M^+(\theta) =& - \alpha E_3(\theta-\theta_T) + (E_1-E_3)M(\theta-\theta_m),
\end{aligned}
\tag{73}
$$

and

$$
\begin{aligned}
\chi_M^-(\theta) =& - \frac{E_1-E_3}{2}[\alpha(\theta-\theta_T)-M(\theta-\theta_m)]^2 \\
\chi_M^+(\theta) =& - \frac{E_1-E_3}{2}[\alpha(\theta-\theta_T)+M(\theta-\theta_m)]^2.
\end{aligned}
\tag{74}
$$

c) For $\theta \in [\theta_I, \theta_m)$

$$
\varrho\psi_R(\varepsilon,\theta) = \varrho C\theta\left(1 - \ ln\frac{\theta}{\theta_T}\right) +
$$

$$
+ \begin{cases} \frac{E_3}{2}\varepsilon^2 + \varepsilon\Sigma_M^-(\theta) + \chi_M^-(\theta) & \text{if } \varepsilon \in [\varepsilon_I(\theta), \varepsilon_m^-(\theta)) \\ -\frac{E_2}{2}\varepsilon^2 + \varepsilon\Sigma_I(\theta) + \chi_I(\theta) & \text{if } \varepsilon \in [\varepsilon_m^-(\theta), \varepsilon_m^+(\theta)] \\ \frac{E_3}{2}\varepsilon^2 + \varepsilon\Sigma_M^+(\theta) + \chi_M^+(\theta) & \text{if } \varepsilon \in (\varepsilon_m^+(\theta), \varepsilon_{II}(\theta)] \end{cases}, \tag{75}
$$

with

$$\begin{array}{l}
\Sigma_M^-(\theta) = -\alpha E_3(\theta-\theta_T) + (E_2+E_3)[M(\theta-\theta_m) - (M-m)(\theta-\theta_M)] \\
\Sigma_I(\theta) = \alpha E_2(\theta-\theta_T) \\
\Sigma_M^+(\theta) = -\alpha E_3(\theta-\theta_T) + (E_2+E_3)[-M(\theta-\theta_m) + (M-m)(\theta-\theta_M)]
\end{array}, \tag{76}$$

and

$$\begin{aligned}
\chi_M^-(\theta) = {} & \frac{E_2+E_3}{2}[\alpha(\theta-\theta_T) + (M-m)(\theta-\theta_M) - M(\theta-\theta_m)]^2 - \\
& \qquad \frac{\alpha^2(E_1+E_2)}{2}(\theta_m-\theta_T)(2\theta-\theta_m-\theta_T) \\
\chi_I(\theta) = {} & -\frac{\alpha^2(E_1+E_2)}{2}(\theta_m-\theta_T)(2\theta-\theta_m-\theta_T) \\
\chi_M^+(\theta) = {} & \frac{E_2+E_3}{2}[\alpha(\theta-\theta_T) - (M-m)(\theta-\theta_M) + M(\theta-\theta_m)]^2 - \\
& \qquad \frac{\alpha^2(E_1+E_2)}{2}(\theta_m-\theta_T)(2\theta-\theta_m-\theta_T)
\end{aligned} . \tag{77}$$

The equilibrium entropy is determined from $(31)_2$.

a) For $\theta \in (\theta_m, \theta_M)$

$$\varrho\eta_R(\varepsilon,\theta) = \varrho C \ \ln\frac{\theta}{\theta_T} +$$

$$\begin{cases}
[-(E_2+E_3)m + (E_1+E_2)M + \alpha E_3]\varepsilon + \Omega_M^-(\theta) & \text{if } \varepsilon \in (\varepsilon_I(\theta), \varepsilon_m^-(\theta)) \\
[(E_1+E_2)M - \alpha E_2]\varepsilon + \Omega^-(\theta) & \text{if } \varepsilon \in (\varepsilon_m^-(\theta), \varepsilon_M^-(\theta)) \\
\alpha E_1 \varepsilon & \text{if } \varepsilon \in (\varepsilon_M^-(\theta), \varepsilon_M^+(\theta)) \\
[-(E_1+E_2)M - \alpha E_2]\varepsilon + \Omega^+(\theta) & \text{if } \varepsilon \in (\varepsilon_M^+(\theta), \varepsilon_m^+(\theta)) \\
[(E_2+E_3)m - (E_1+E_2)M + \alpha E_3]\varepsilon + \Omega_M^+(\theta) & \text{if } \varepsilon \in (\varepsilon_m^+(\theta), \varepsilon_{II}(\theta))
\end{cases}, \tag{78}$$

with the notations

$$\begin{aligned}
\Omega_M^-(\theta) = {} & (M-\alpha)(E_1+E_2)[M(\theta-\theta_m) - \alpha(\theta-\theta_T)] \\
& - (m-\alpha)(E_2+E_3)[M(\theta-\theta_m) + (m-M)(\theta-\theta_M) - \alpha(\theta-\theta_T)] \\
\Omega^-(\theta) = {} & (M-\alpha)(E_1+E_2)[M(\theta-\theta_m) - \alpha(\theta-\theta_T)] \\
\Omega^+(\theta) = {} & (M+\alpha)(E_1+E_2)[M(\theta-\theta_m) + \alpha(\theta-\theta_T)] \\
\Omega_M^+(\theta) = {} & (M+\alpha)(E_1+E_2)[M(\theta-\theta_m) + \alpha(\theta-\theta_T)] \\
& - (m+\alpha)(E_2+E_3)[M(\theta-\theta_m) + (m-M)(\theta-\theta_M) + \alpha(\theta-\theta_T)]
\end{aligned} . \tag{79}$$

b) For $\theta \in (\theta_M, \theta_{II})$

$$\varrho\eta_R(\varepsilon,\theta) = \varrho C \ \ln\frac{\theta}{\theta_T} +$$

$$\begin{cases} [(E_1 - E_3)M + \alpha E_3]\varepsilon + \Omega_M^-(\theta) & \text{if } \ \varepsilon \in (\varepsilon_I(\theta), \varepsilon_M^-(\theta)) \\ \alpha E_1 \varepsilon & \text{if } \ \varepsilon \in (\varepsilon_M^-(\theta), \varepsilon_M^+(\theta)) \\ [-(E_1 - E_3)M + \alpha E_3]\varepsilon + \Omega_M^+(\theta) & \text{if } \ \ \varepsilon \in (\varepsilon_M^+(\theta), \varepsilon_{II}(\theta)) \ , \end{cases} \tag{80}$$

with

$$\begin{aligned} \Omega_M^-(\theta) =& - (M - \alpha)(E_1 - E_3)[\alpha(\theta - \theta_T) - M(\theta - \theta_m)] \\ \Omega_M^+(\theta) =& (M + \alpha)(E_1 - E_3)[\alpha(\theta - \theta_T) + M(\theta - \theta_m)]. \end{aligned} \tag{81}$$

c) For $\theta \in (\theta_I, \theta_m)$

$$\varrho\eta_R(\varepsilon,\theta) = \varrho C \ \ln\frac{\theta}{\theta_T} +$$

$$\begin{cases} [-(E_2 + E_3)m + \alpha E_3]\varepsilon + \Omega_M^-(\theta) & \text{if } \ \varepsilon \in (\varepsilon_I(\theta), \varepsilon_m^-(\theta)) \\ -\alpha E_2 \varepsilon + \Omega_I(\theta) & \text{if } \ \varepsilon \in (\varepsilon_m^-(\theta), \varepsilon_m^+(\theta)) \\ [(E_2 + E_3)m + \alpha E_3]\varepsilon + \Omega_M^+(\theta) & \text{if } \ \ \varepsilon \in (\varepsilon_m^+(\theta), \varepsilon_{II}(\theta)) \ , \end{cases} \tag{82}$$

with

$$\begin{aligned} \Omega_M^-(\theta) &= (m - \alpha)(E_2 + E_3)[\alpha(\theta - \theta_T) + (M - m)(\theta - \theta_M) - M(\theta - \theta_m)] + \\ &\qquad \alpha^2(E_1 + E_2)(\theta_m - \theta_T) \\ \Omega_I(\theta) &= \alpha^2(E_1 + E_2)(\theta_m - \theta_T) \\ \Omega_M^+(\theta) &= -(m + \alpha)(E_2 + E_3)[\alpha(\theta - \theta_T) - (M - m)(\theta - \theta_M) + M(\theta - \theta_m)] + \\ &\qquad \alpha^2(E_1 + E_2)(\theta_m - \theta_T) \end{aligned} . \tag{83}$$

Since in the next section we investigate the capability of the model to describe stress-induced $A \rightleftharpoons M^+$ phase transitions only we give bellow a partial description of the free energy function $\psi = \hat{\psi}(\varepsilon, \sigma, \theta)$ of the thermo-viscoelastic model, as it was deduced in [] in the domain $\{(\varepsilon, \theta, \sigma = E\varepsilon + h(\tilde{\varepsilon}, \theta))/\varepsilon, \tilde{\varepsilon} \in (\varepsilon_I(\theta), \varepsilon_{II}(\theta)), \theta \in (\theta_m, \theta_M)\}$.

$$\varrho\hat{\psi}(\varepsilon, \sigma, \theta) = \frac{\sigma^2}{2E} + \frac{\alpha^2 E_1^2}{2(E - E_1)}(\theta - \theta_T)^2 + \varrho\theta C(1 - \ln(\theta/\theta_T)) +$$

$$
\begin{cases}
\frac{E_1}{2E(E-E_1)}(\sigma - E\varepsilon)^2 + \frac{\alpha^2 E_1}{(E-E_1)}(\theta-\theta_T)(\sigma - E\varepsilon), \\
\qquad\qquad\qquad\qquad \text{if } \ \tau_M^+(\theta) \le \sigma - E\varepsilon \le \tau_M^-(\theta), \\
-\frac{E_2}{2E(E+E_2)}(\sigma - E\varepsilon)^2 + \varphi_1(\theta) \\
-\left[\frac{\alpha E_2}{(E+E_2)}(\theta-\theta_T) + \frac{(E_1+E_2)M}{(E+E_2)}(\theta-\theta_m)\right](\sigma - E\varepsilon), \\
\qquad\qquad\qquad\qquad \text{if } \ \tau_m^+(\theta) < \sigma - E\varepsilon < \tau_M^+(\theta), \\
\frac{E_3}{2E(E-E_3)}(\sigma - E\varepsilon)^2 + \varphi_2(\theta) + \frac{(\sigma-E\varepsilon)}{(E-E_3)}[\alpha E_3(\theta-\theta_T) - \\
(E_2+E_3)(M-m)(\theta-\theta_M) - (E_1-E_3)M(\theta-\theta_m)], \\
\qquad\qquad\qquad\qquad \text{if } \ \sigma - E\varepsilon \le \tau_m^+(\theta),
\end{cases}
\tag{84}
$$

where

$$
\begin{aligned}
\varphi_1(\theta) =& -\frac{(E_1+E_2)}{2(E+E_2)(E-E_1)}[\alpha E(\theta-\theta_T) + (E-E_1)M(\theta-\theta_m)]^2 \\
\varphi_2(\theta) =& \varphi_1(\theta) + \frac{(E_2+E_3)}{2(E+E_2)(E-E_3)}[\alpha E(\theta-\theta_T) + (E-E_1)M(\theta-\theta_m) \\
& -(E+E_2)(M-m)(\theta-\theta_M)]^2
\end{aligned}
\tag{85}
$$

and

$$
\begin{aligned}
\tau_M^-(\theta) =& (E-E_1)M(\theta-\theta_m) - \alpha E(\theta-\theta_T) \\
\tau_M^+(\theta) =& -(E-E_1)M(\theta-\theta_m) - \alpha E(\theta-\theta_T)\,. \\
\tau_m^+(\theta) =& \tau_M^+(\theta) + (E+E_2)(M-m)(\theta-\theta_M)
\end{aligned}
\tag{86}
$$

It is also important to write the expression of the equilibrium heat capacity at constant strain which is piecewise continuous.

a) For $\theta \in (\theta_m, \theta_M)$

$$
C_R(\varepsilon,\theta) \equiv -\theta \frac{\partial^2 \psi_R}{\partial \theta^2}(\varepsilon,\theta) = C +
$$

$$
+\begin{cases}
\theta/\varrho[(M-\alpha)^2(E_1+E_2) - (m-\alpha)^2(E_2+E_3)] & \text{if} \quad \varepsilon \in (\varepsilon_I(\theta), \varepsilon_m^-(\theta)) \\
\theta/\varrho(M-\alpha)^2(E_1+E_2) & \text{if} \quad \varepsilon \in (\varepsilon_m^-(\theta), \varepsilon_M^-(\theta)) \\
0 & \text{if} \quad \varepsilon \in (\varepsilon_M^-(\theta), \varepsilon_M^+(\theta)) \\
\theta/\varrho(M+\alpha)^2(E_1+E_2) & \text{if} \quad \varepsilon \in (\varepsilon_M^+(\theta), \varepsilon_m^+(\theta)) \\
\theta/\varrho[(M+\alpha)^2(E_1+E_2) - (m+\alpha)^2(E_2+E_3)] & \text{if} \quad \varepsilon \in (\varepsilon_m^+(\theta), \varepsilon_{II}(\theta)).
\end{cases}
\tag{87}
$$

b) For $\theta \in (\theta_M, \theta_{II})$

$$
C_R(\varepsilon,\theta) = C + \begin{cases}
\theta/\varrho(M-\alpha)^2(E_1-E_3) & \text{if} \quad \varepsilon \in (\varepsilon_I(\theta), \varepsilon_M^-(\theta)) \\
0 & \text{if} \quad \varepsilon \in (\varepsilon_M^-(\theta), \varepsilon_M^+(\theta)) \\
\theta/\varrho(M+\alpha)^2(E_1-E_3) & \text{if} \quad \varepsilon \in (\varepsilon_M^+(\theta), \varepsilon_{II}(\theta))
\end{cases} .
\tag{88}
$$

c) For $\theta \in (\theta_I, \theta_m)$

$$C_R(\varepsilon,\theta) = C - + \begin{cases} \theta/\varrho(m-\alpha)^2(E_2+E_3) & \text{if} \quad \varepsilon \in (\varepsilon_I(\theta), \varepsilon_m^-(\theta)) \\ 0 & \text{if} \quad \varepsilon \in (\varepsilon_m^-(\theta), \varepsilon_m^+(\theta)) \\ \theta/\varrho(m+\alpha)^2(E_2+E_3) & \text{if} \quad \varepsilon \in (\varepsilon_m^+(\theta), \varepsilon_{II}(\theta)) \end{cases} . \quad (89)$$

The equilibrium heat capacity $C_R(\varepsilon,\theta)$ is different from the value at equilibrium of the non-equilibrium heat capacity $C(\varepsilon,\theta,\sigma)$ defined by (21) (compare to relations (30) and (31) for the free energy and entropy).

The coefficient of thermal expansion of the thermoelastic constitutive equation we propose here, i.e. $-\frac{\partial^2\hat{\psi}_R}{\partial\varepsilon\partial\theta}/\frac{\partial^2\hat{\psi}_R}{\partial\varepsilon^2}$ is a piecewise constant function on its domain of definition. For instance, on the A-region ($\varepsilon \in [\varepsilon_M^-(\theta), \varepsilon_M^+(\theta)]$) it is equal to α, on I^+-region ($\varepsilon \in [\varepsilon_M^+(\theta), \varepsilon_m^+(\theta)],$) it is equal to $\alpha + M(1+E_1/E_2)$, while on M^+-region ($\varepsilon > \varepsilon_m^+(\theta)$) it is equal to $\alpha + m(E_3+E_2)/E_3 - M(E_1 + E_2)/E_3$.

Let us note that since the thermoelastic constitutive relation is only continuous in strain and temperature, the PDEqs system (20) is one with discontinuous coefficients on their domain of definition.

6 Numerical approach: coupled strain - temperature analysis

We now describe some numerical simulations of a loading-unloading strain controlled experiment interrupted by a relaxation one. They illustrate the capability of our model to capture the nucleation and propagation of strain fields in thin bars under uniaxial tension and the corresponding severe thermomechanical interactions seen in pseudoelastic NiTi shape memory alloys (see Shaw and Kyriakides, 1997).

Phase transformation phenomena observed in shape memory alloys are typical examples of evolving material instabilities. It is known that the initiation locus of the transformed material (strain bands) in such materials is very sensitive to any slight disturbances although the propagation and global measurements (as stress vs. overall strain) always exhibit the same trends. Some time in laboratory experiments (see for example Ward and Holliday (1975)) the point of initiation of the new phase is quite variable in bars of uniform cross-section. To avoid such inconvenience in the study of propagation fronts a very small geometric defect is made in the specimen to fix the initiation locus of the strain band (see for instance Grenet and G'Sell, 1990) who reduce the thickness of the specimen by about 1% in a small area).

We are here interested to investigate what our model and numerical method predict when we simulate a hard testing machine experiment on a slightly non-uniform bar of the type described in Section 2 (the case of a uniform bar was investigated in Făciu and Mihăilescu-Suliciu, 2002a). We take in the following a small value of the geometrical parameter entering Section 2.1, i.e., $a = 10^{-2}$ which corresponds to a reduction of the thickness of the cross-sectional area of the specimen by about 0.04%.

We consider the bar initially at rest, unstressed at a temperature $\theta_0 \in [\theta_m, \theta_M]$ for which the material is in the austenitic phase. We also suppose $\sigma_m(\theta_0) > 0$ which is a necessary condition for a pseudoelastic material response of the material. The bar, firmly fixed at one end, is subjected to a traction-compression test with a constant velocity v^*. Between the loading and the unloading experiment we simulate a pause, during which both ends of the specimen are fixed, i.e., the length of the bar is maintained constant (relaxation experiment).

The ambient temperature around the specimen is assumed to be constant and equal to $\theta_0 = 310.{}^0K$.

We describe the analysis associated with these loading conditions in some details while the analysis corresponding to other thermo-mechanical loading tests as stress- and temperature-controlled problems has been presented in Făciu and Mihăilescu-Suliciu, (2002b), (2002c).

Thus we consider for the PDEqs's system (20) the following initial boundary value problem which corresponds to a strain controlled problem with Newton's type convection mode of heat transfer at the ends of the specimen

$$\begin{aligned}
&(\varepsilon, \sigma, v, \theta)(X, 0) = (0, 0, 0, \theta_0), \qquad \text{for any } X \in [0, L],\\
&v(0, t) = v^*, \qquad v(L, t) = 0, \quad \text{for any } \ t \in [0, t_1)\\
&v(0, t) = 0, \quad v(L, t) = 0, \quad \text{for any } \ t \in [t_1, t_2)\\
&v(0, t) = -v^*, \quad v(L, t) = 0, \quad \text{for any } \ t \in [t_2, t_3).
\end{aligned} \tag{90}$$

$$-\kappa \frac{\partial \theta}{\partial X}(0, t) = -\omega^*(\theta(0, t) - \theta_0), \qquad -\kappa \frac{\partial \theta}{\partial X}(L, t) = \omega^*(\theta(L, t) - \theta_0) \text{ for any } t > 0.$$

Here the heat exchange coefficient ω^* is much larger than ω, since it characterizes the heat transfer between the bar and the grips of the testing machine while ω characterizes the heat transfer transfer between the bar and its environment which is supposed a much less convective medium. Very large values of ω^* approximate in fact isothermal end conditions. We used in the following $\omega^* = 40000.W/m^2/{}^0K$ and $\omega = 250.W/m^2/{}^0K$.

In order to study the qualitative prediction of our model we choose realistic values of the material parameters appropriate for a Cu-Zn-Ni shape memory alloy (see for instance Abeyaratne et al. (1994) and Făciu and Mihăilescu-Suliciu (2002a)). We used the following numerical entries:

$$\begin{aligned}
&E = 31.5GPa, \quad E_1 = 30.GPa, \quad E_2 = 0.5GPa, \quad E_3 = 22.GPa, \\
&k = 10^4/s, \quad \rho = 8000.Kg/m^3, \\
&\alpha = 1.8 \times 10^{-6}/^0C, \quad \kappa = 20.W/m/^0C, \quad C = 400.J/Kg/^0C, \\
&\theta_m = 280.\ ^0K, \quad \theta_M = 10000.\ ^0K, \quad \theta_T = 283.3\ ^0K, \\
&M = 10.1371 \times 10^{-5}/^0C, \quad m = 9.7253 \times 10^{-5}/^0C
\end{aligned} \tag{91}$$

Like in Abeyaratne et al. (1994), the reference temperature $\theta_T \in (\theta_m, \theta_M)$ used in our numerical entries (91) has the property that the Maxwell stress for $(A) \rightleftharpoons (M)$ transformations is zero at $\theta = \theta_T$, and we call it the transformation temperature.

For the above input data the stress required for $(A) \to (M^+)$ transformation increases at the rate $\frac{d\sigma_M(\theta)}{d\theta} = 3.04113MPa/^0C$, while the stress required for the reverse transformation $(M^+) \to (A)$ changes at the rate $\frac{d\sigma_m(\theta)}{d\theta} = 3.04114MPa/^0C$.

In order to investigate the influence of the loading rates on the strain and temperature distribution into the specimen during direct $(A) \to (M)$ and reverse $(M) \to (A)$ phase transformations two numerical experiments has been performed at constant strain rates $\dot{\varepsilon}_e = v^*/L$ equal to $5 \times 10^{-2}/sec$ and $5 \times 10^{-3}/sec$, respectively.

To obtain the numerical solution for the above initial-boundary value problem we built a first-order approximation scheme. The relation between the time integration step Δt and the mesh size ΔX is $\Delta X = \sqrt{E/\rho}\Delta t$, where Δt verifies some numerical stability conditions which will be analyzed elsewhere. In the numerical experiments presented below we have used 401 nodes on the interval [0,L].

One of the aim of this paper is to illustrate the agreement between our thermo-viscoelastic constitutive modeling of shape memory alloys and laboratory observations.

Therefore, we compare the numerical results with laboratory experiments performed by Shaw and Kyriakides (1997) in studying the nucleation and propagation of phase transformation fronts in a NiTi alloy. Their experimental methodology consist in simultaneous full field monitoring of the deformation and thermal changes in NiTi during mechanically unstable regimes associated with the pseudoelastic material response. In order to do that, they apply a brittle ceramic coating on the surface of the strip which tends to shatter when subjected to significant strain changes such as those associated with $(A) \leftrightarrow (M)$ transformations. This results in surface relief and reflectivity changes which under favorable lighting conditions are seen by the naked eye as a change in color: black regions representing untransformed material (A) and shiny regions representing transformed material (M). This property of the coating was used to monitor the inhomogeneous evolution of the strain. The events were recorded by a photographic camera programmed to take photographs at preselected time intervals. Since the evolution of phase transformations in NiTi is strongly influenced by the emmission/absorbtion of latent heats which results in self-heating/cooling of the material a full field view of the temperature distribution in the test section was recorded by using infrared imaging technique. Thus the thermal camera converts the signal into calibrated color contours which are recorded at the same time intervals as the optical images. In order to explain the events that take place during stress-induced $(A) \leftrightarrow (M)$ transformations they correlate the optical images (strain distribution), the thermal images (temperature distribution) with the stress history.

The same as in laboratory experiments in our numerical tests, we simultaneously record and examine the strain and temperature distribution in the bar as well as the end-stress $\sigma(0,t)$ versus the engineering strain $\varepsilon_e(t) = \frac{1}{L}\int_0^L \varepsilon(X,t)dX$ where according to (90) $\dot{\varepsilon}(t) = -v^*/L$=const. Moreover, we represent the evolution of the two phases as well as their thermal behavior in the same form as in the laboratory experiments, that is converting the numerical values in a scale of colors.

Numerical simulation 1: $\dot{\varepsilon}_e = v^*/L = 5 \times 10^{-2}/sec$

Loading: $(A) \rightarrow (M)$ *transformation*

In this experiment we have selected from the loading record of numerical data a sequence of 23 times separated by 0.038s intervals marked with empty circles on the stress-engineering strain curve (Fig. 6). The corresponding configurations of the strain and temperature distribution in the specimen describing the $(A) \rightarrow (M)$ transformation are represented in Fig. 7 and Fig. 8, respectively.

Upon loading, the material in the austenite phase deforms practically thermo-elastically, the deformation in the specimen is homogeneous [1 in Fig. 7] and the corresponding temperature [1 in Fig. 8] is essentially uniform and equal to the ambient temperature (310^0K). In image 2 of Fig. 8 we note that the temperature at the middle of the specimen has risen slightly to $311.^0K$ (blue - green) and corresponds to the region where the value of the deformation

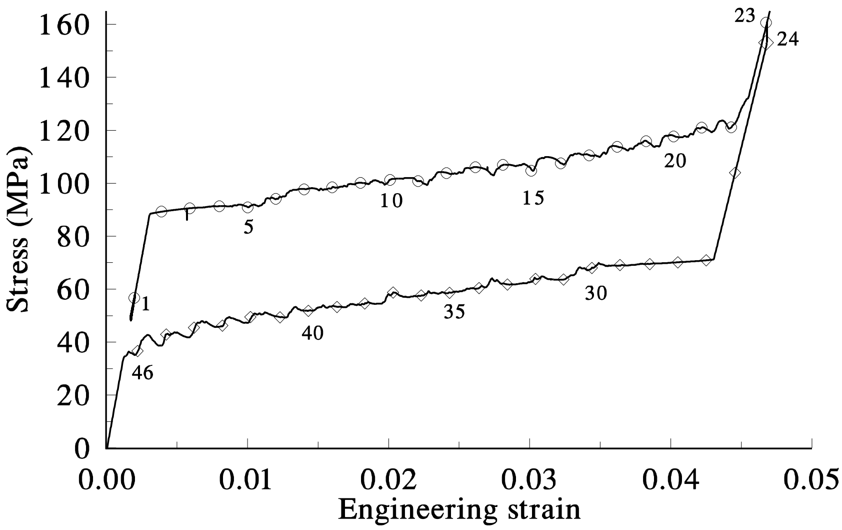

Figure 6: Strain-controlled hysteresis loop at $\dot{\varepsilon}_e = 10^{-2}/s$

increases. The nucleation zone is much more visible in configuration 3 which is accompanied by an increase in temperature until $312.5^0 K$.

In configuration 4 the transformation of the material (strain localization) is already complete in four zones, symmetric with respect to the middle of the bar, while multiple nucleation points of the new phase are still visible. Afterwards some interfaces are arrested (stationary phase boundaries) while others propagate. One can observe that as the fronts propagate the hot zones in Fig. 8 spread and the local temperatures increase. Clearly, at this displacement rate heat transfer to the environment cannot keep up with the rate at which latent heat is released by the material. As the temperature increases so does the stress, so that by 22 it has risen to 120MPa. We can observe some oscillations on the horizontal plateau of the hysteresis loop which reflect the nucleation and propagation of phase boundaries during the transformation (unstable thermomechanical behavior). A detailed analysis of this phenomenon has been done in Făciu and Mihăilescu-Suliciu (2002a). During the end of the transformation (see images 18 to 22 of Fig. 8) the heat fluxes from adjacent fronts begin to interact significantly and local heating intensifies. The temperature over the most of the specimen climbs to $322.^0 K$ (white - red). Beyond the time 22 (Fig. 6-8) the deformation is homogeneous, the stress rises at a significantly higher rate and the temperature starts to return to ambient. Loading is terminated at time 23.

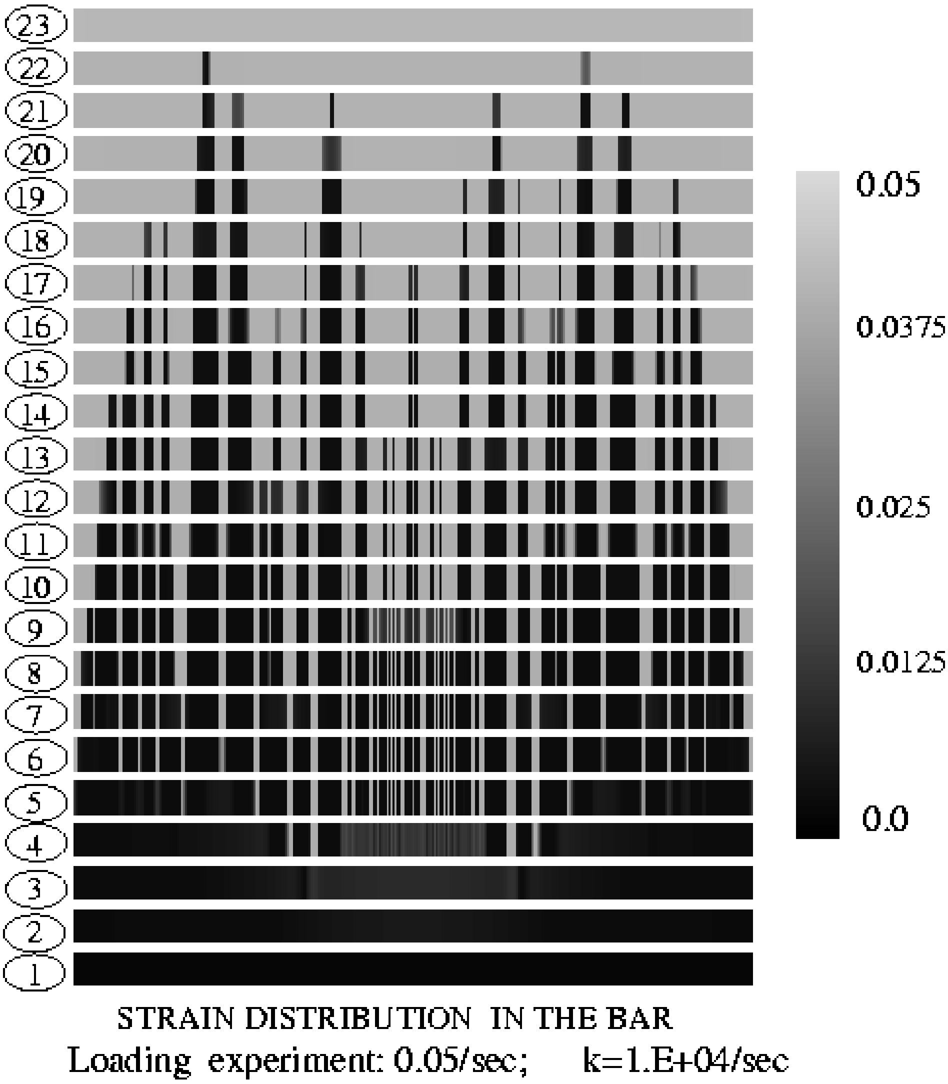
23
22
21
20
19
18
17
16
15
14
13
12
11
10
9
8
7
6
5
4
3
2
1
0.05
0.0375
0.025
0.0125
0.0
STRAIN DISTRIBUTION IN THE BAR
Loading experiment: 0.05/sec; k=1.E+04/sec

Figure 7:

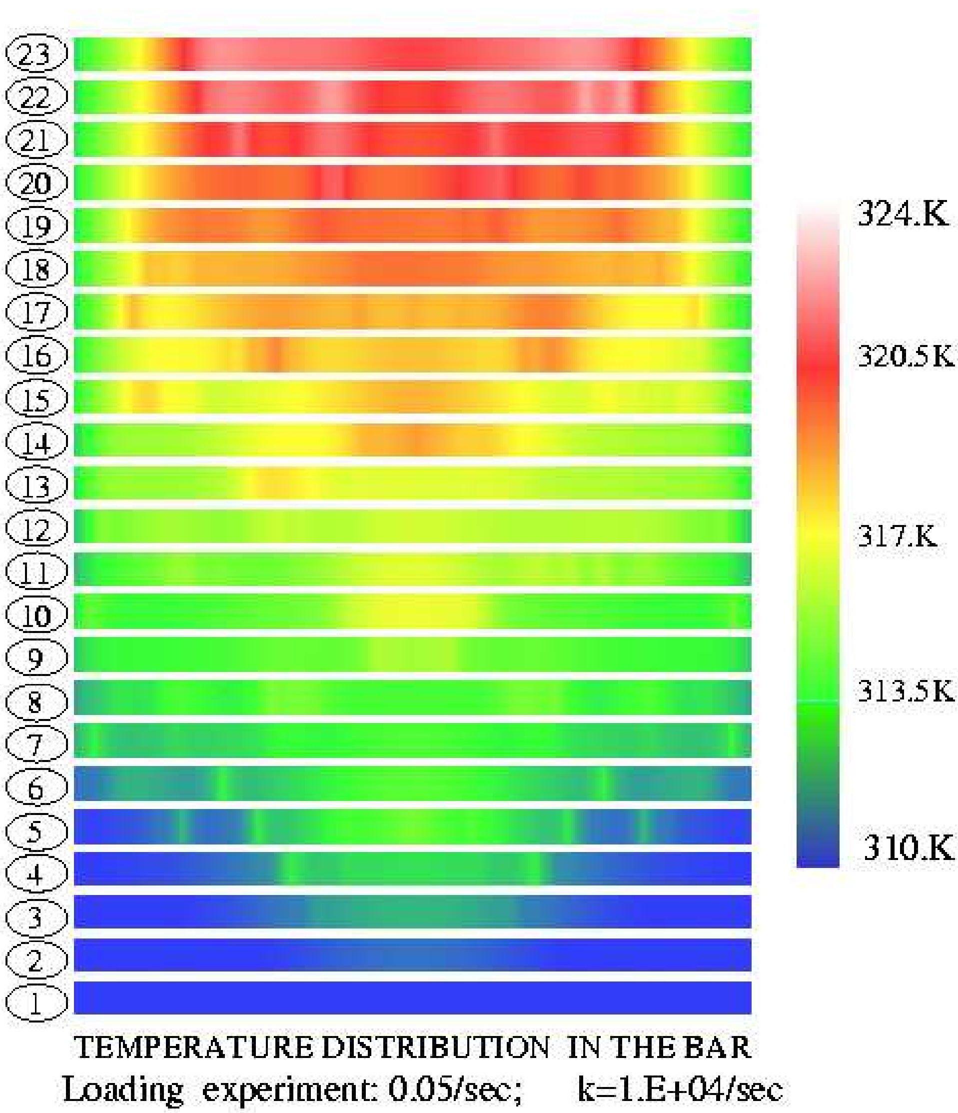
23
22
21
20
19
18
17
16
15
14
13
12
11
10
9
8
7
6
5
4
3
2
1
324.K
320.5K
317.K
313.5K
310.K
TEMPERATURE DISTRIBUTION IN THE BAR
Loading experiment: 0.05/sec; k=1.E+04/sec

Figure 8:

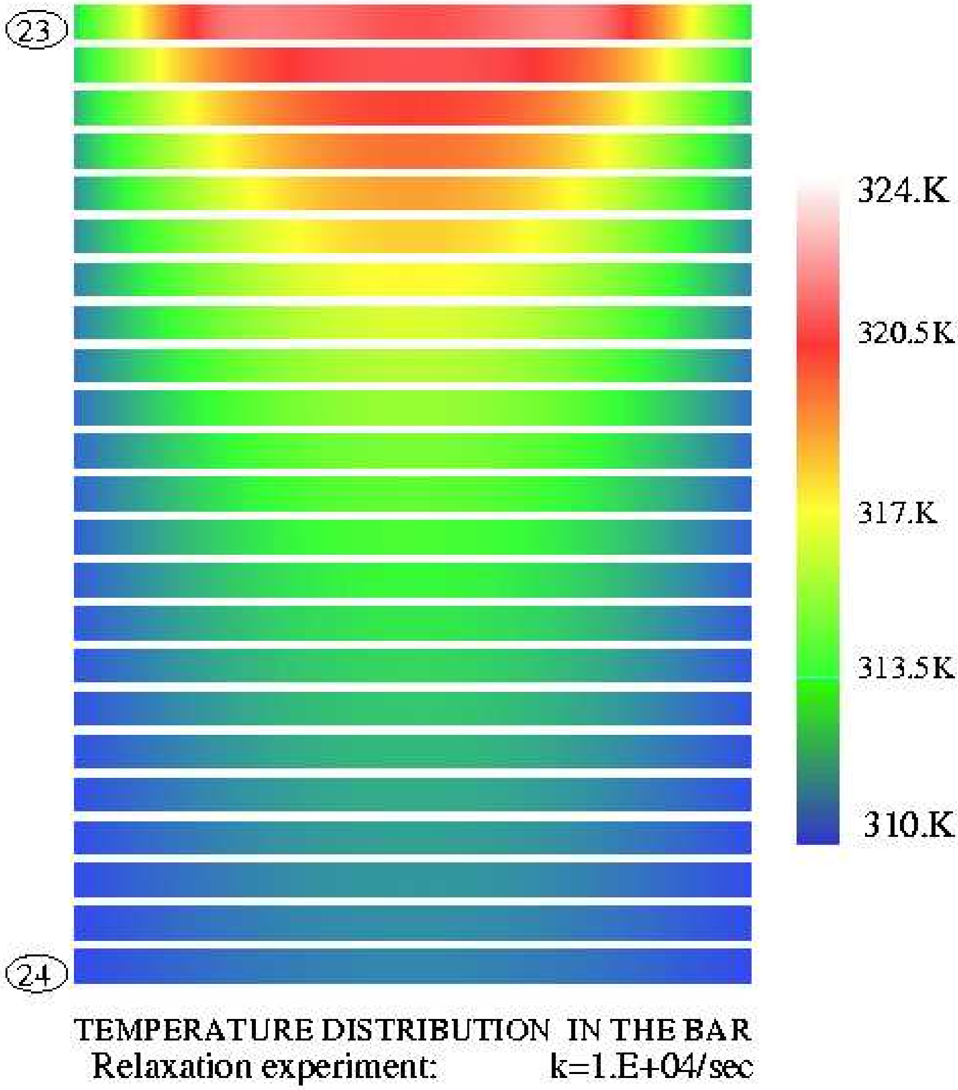
23
24
324.K
320.5K
317.K
313.5K
310.K
TEMPERATURE DISTRIBUTION IN THE BAR
Relaxation experiment: k=1.E+04/sec

Figure 9:

Since this test is conducted at a high enough displacement rate multiple nucleations of the new phase occur resulting in the coexistence and simultaneous propagation of several phase transformation fronts. Therefore, the thermal sequence show severe self-heating due to the lack of time for convection and radiation to manifest. Thus, the difference between the maximal value of temperature in the bar at the end of the loading process and the ambient temperature is about $14^0 K$ (see the temperature legend).

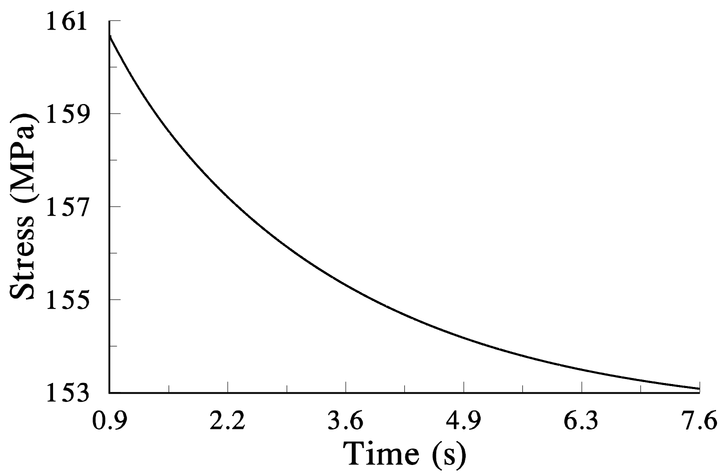

Figure 10: Relaxation of the end-stress $\sigma(0,t)$ between times 23 and 24.

Relaxation.

Between the times 23 and 24 we simulate a relaxation experiment maintaining fixed the ends of the bars 6.7s. The end-stress $\sigma(0,t)$ decreases from 160.68MPa to 153.074MPa (Fig. 10) while the specimens temperature decreases in the middle of the bar from $322.^0 K$ to $311.^0 K$ (Fig. 9). Let us note that the relaxation of the stress as it is described by the present approach is due mainly to the thermomechanical coupling and to the heat transfer between the bar and its surrounding and not especially to the viscosity incorporated in the model. This is in agreement with the experimental observation (see Shaw (2000)) that the "rate effect" in the material is not the usual viscoelastic phenomena, but rather, a strong interaction between the latent heat of transformation and the material's extreme sensitivity to temperature. Relaxation processes are also predicted by the shape memory model used by Balandraud et al. (2000) (see also the references therein) when including the thermo-mechanical coupling of the material with its environment.

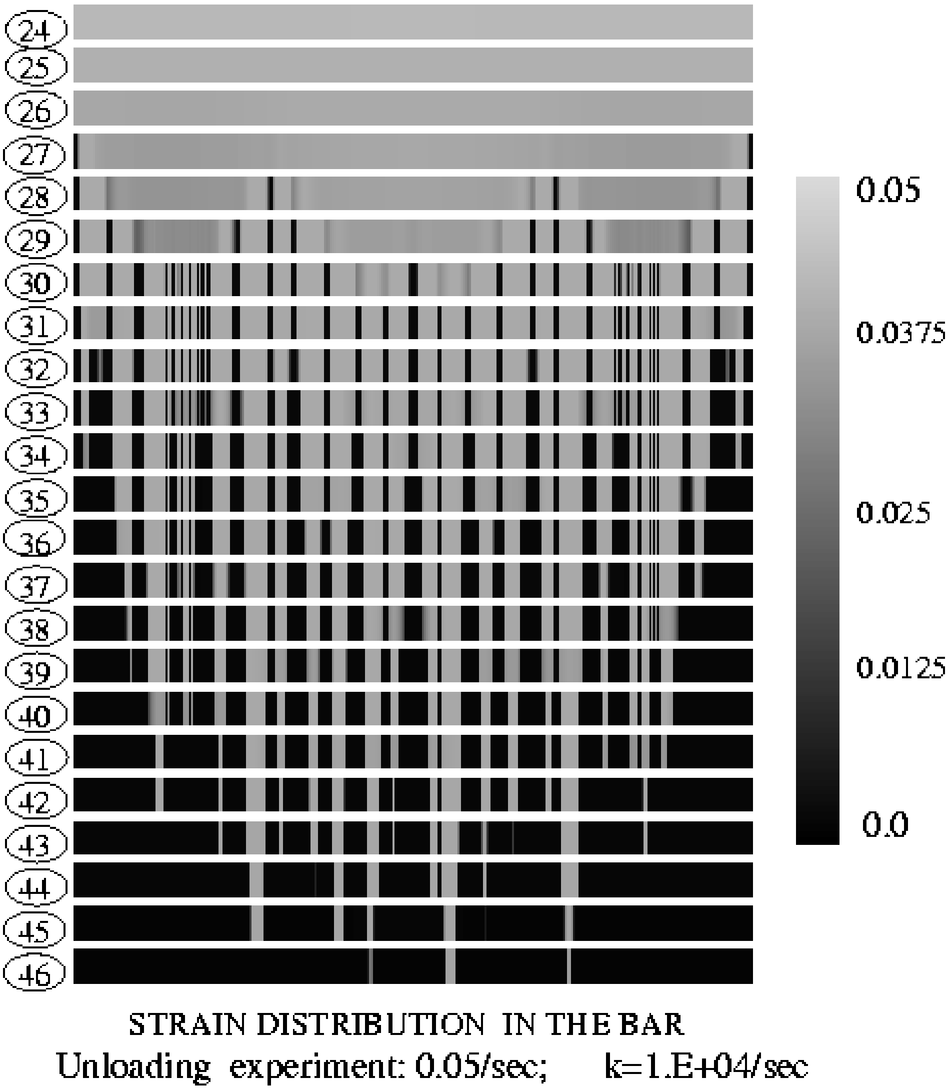
24
25
26
27
28
29
30
31
32
33
34
35
36
37
38
39
40
41
42
43
44
45
46
0.05
0.0375
0.025
0.0125
0.0
STRAIN DISTRIBUTION IN THE BAR
Unloading experiment: 0.05/sec; k=1.E+04/sec

Figure 11:

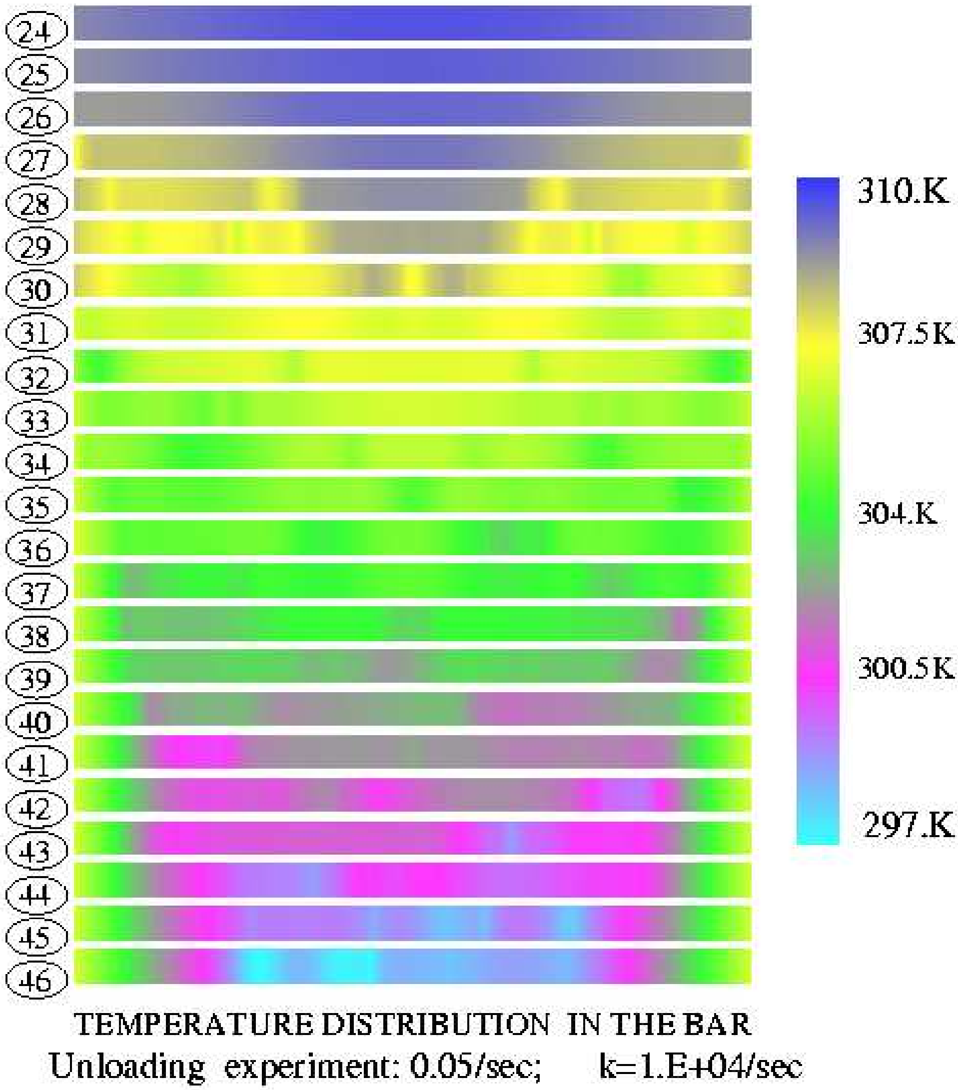
24
25
26
27
28
29
30
31
32
33
34
35
36
37
38
39
40
41
42
43
44
45
46
310.K
307.5K
304.K
300.5K
297.K
TEMPERATURE DISTRIBUTION IN THE BAR
Unloading experiment: 0.05/sec; k=1.E+04/sec

Figure 12:

Unloading: $(M) \rightarrow (A)$ transformation.

Unloading commences at time 24 and the stress decreases linearly with respect to the engineering strain while the deformation is homogeneous in the (M) phase and the temperature continue to return to the ambient (linear thermoelastic behavior). In 25 [Fig. 12] the middle of the specimen is still warmer than its extremities since we left not enough time to the specimen to release by radiation the heat accumulated during the exothermic $(A) \rightarrow (M)$ transformation. At time 26 we observe a slightly decrease of the temperature at the ends of the specimen (light blue) below the ambiental one (about $1^0 K$) which prefigures the site where the austenite first appears in configuration 27. Thus nucleation events are now accompanied by a cooling of the corresponding locations. The temperature of the specimen becomes progressively colder. At 34 where we have a regular distribution of the two phase into the specimen we also have an almost uniform temperature (green) of about $304.^0 K$ excepting the extremities were we have practically isothermal end conditions. After each coalescence of the fronts the cooling rate intensifies [41 to 46 in Fig. 12] thereby further lowering the local temperatures and further decreasing the stress. Just after 46 the whole specimen has reverted to (A) and the numerical experiment is terminated after the last elastic unloading.

Numerical simulation 2: $\dot{\varepsilon}_e = v^*/L = 5 \times 10^{-3}/sec$

We present here only the loading part of the hysteresis loop. In this experiment we also have represented 23 successive configurations of the strain and temperature distribution in the specimen separated now by 0.38s (Figs. 14-15). These synchronized images which describes the nucleation and propagation of transformation fronts correspond to 23 positions on the saw-tooth like stress-engineering strain curve in Fig. 13. The results obtained in this test in which the specimen is loaded at the same ambiental temperature but at a rate ten times slower as the previous one is in agreement with experimental observations reported by Shaw and Kyriakides (1997). Thus the number of nucleated and propagating fronts is much lower in the case of lower loading rates.

Like in laboratory experiments smaller temperature peaks (yellow or red spots) in Fig. 15 correspond just to a nucleation site or to a propagating front. Afterwards the temperature diffuses in the bar through axial conduction and to the environment through lateral radiation. The nucleation sites of the (M) phase appear again symmetrically with respect to the middle of the specimen (geometrical effect) and further on its localized at its ends (effect of thermal boundary conditions) (Fig. 14-15). The calculated thermal sequence shows

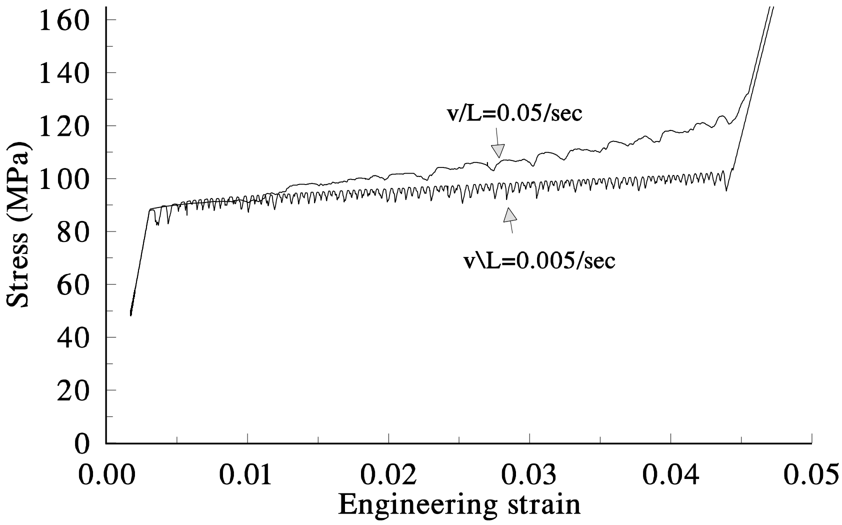

Figure 13: Influence of the strain-rate on the upper branch of the hysteresis loop

a general rise in temperature as the fronts travel, approach each other and consequently thermally interact. When the transformation is complete the temperature tends to return to the ambient [compare 22 to 23 in Figs. 15]. During this time the level of the peaks of the sawtooth-like stress-engineering strain curve rises continuously.

The kinematic differences between the two numerical simulations have a corresponding effect on the recorded end-stress vs. engineering strain response. Thus, the number of stress drops on the horizontal plateau of the hysteresis loop increase for a slower displacement rate. In tests at higher end-displacement rates the tooth of a stress-drop is smoothed while the global load-deformation response maintained an almost positive slope.

Such a behavior is in agreement with laboratory experiments. For example, a seemingly stabilized stress-strain behavior (almost positive tangent) is observed under faster loading rate or a relatively nonconvective medium, like air (see Shaw (2000)). It should be also noted that this behavior is opposite to the destabilizing effects of temperature rise during adiabatic shear band in more conventional materials (Molinari and Clifton, (1987)).

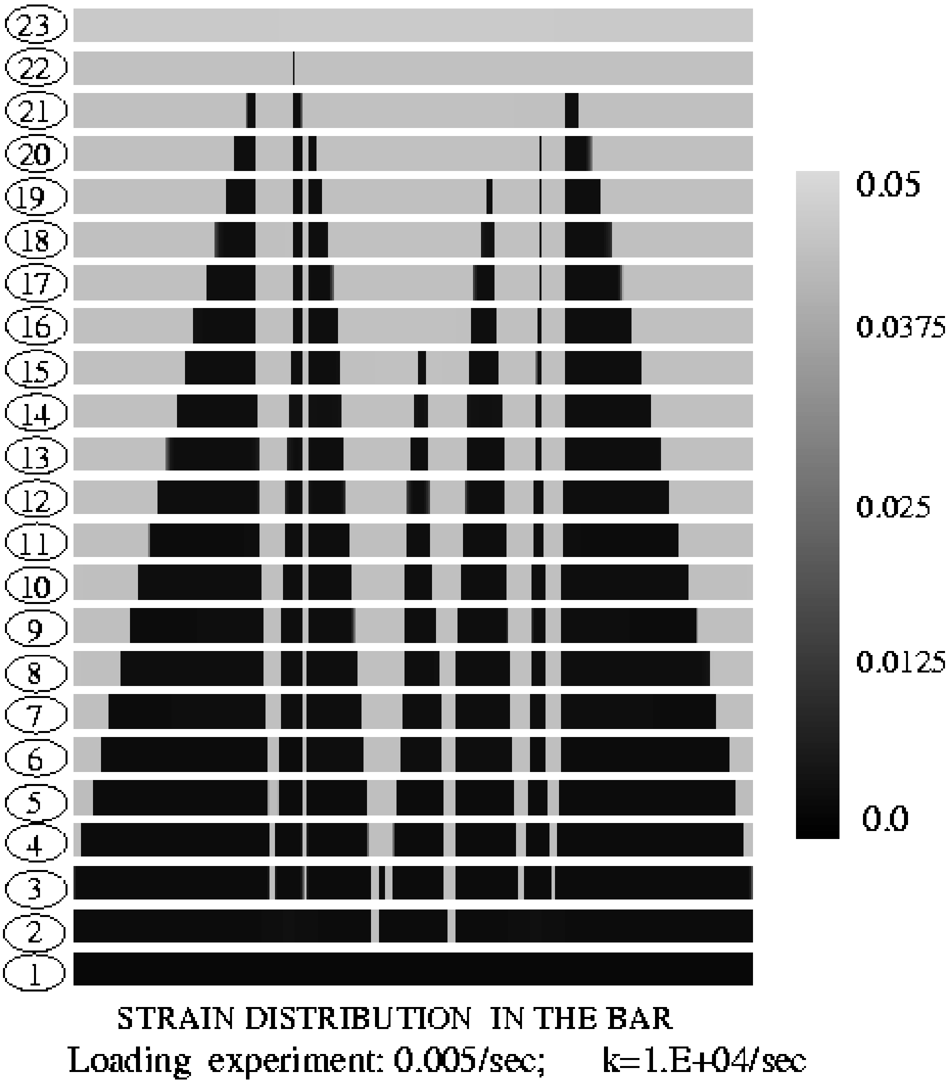
23
22
21
20
19
18
17
16
15
14
13
12
11
10
9
8
7
6
5
4
3
2
1
0.05
0.0375
0.025
0.0125
0.0
STRAIN DISTRIBUTION IN THE BAR
Loading experiment: 0.005/sec; k=1.E+04/sec

Figure 14:

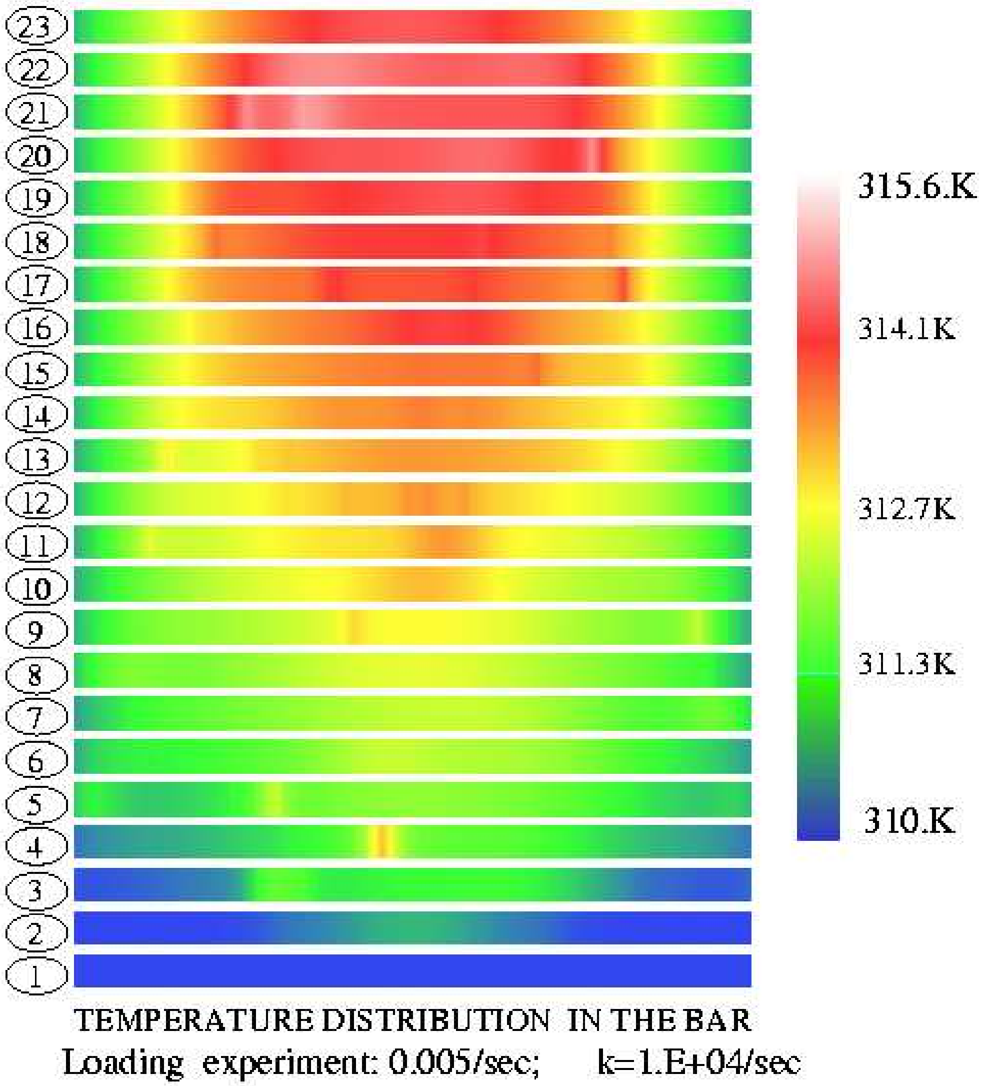
23
22
21
20
19
18
17
16
15
14
13
12
11
10
9
8
7
6
5
4
3
2
1
315.6.K
314.1K
312.7K
311.3K
310.K
TEMPERATURE DISTRIBUTION IN THE BAR
Loading experiment: 0.005/sec; k=1.E+04/sec

Figure 15:

7 Acknowledgement

This research has partially be done in the frame of the scientific Co-operation program between Eastern Europe and Switzerland (SCOPES 2000 - 2003).

References

[1] Abeyaratne, R. and Knowles, J. K. (1991) Implications of viscosity and strain-gradient effects for the kinetics of propagating phase boundaries in solids, *SIAM J. Appl. Math.*, **51**, 1205-1221.

[2] Abeyaratne, R. and Knowles, J. K. (1993) A continuum model of a thermoelastic solid capable of undergoing phase transitions, *J. Mech. Phys. Solids*, **41**, 541-571.

[3] Abeyaratne, R., Kim, S.-J. and Knowles, J. K. (1994) A one-dimensional continuum model for shape memory alloys, *Int. J. Solids Structures*, **31**, 2229-2249.

[4] Bruno, O. P. (1995) Quasistatic dynamics and pseudoelasticity in polycrystalline shape memory wires, *Smart Mater. Struct.*, **4**, 7-13.

[5] Balandraud, X., Ernst E. and Soós, E. (2000) Relaxation and creep phenomena in shape memory alloys. Part I: Hysteresis loop and pseudoelastic behavior. Part II: Stress relaxation and strain creep during phase transformation., *Z. angew. Math. Phys.*, **51**, 171-203, 419-448.

[6] Ball, J.M. and James R.D., (1987) Fine phase mixtures as minimizers of energy., *Arch. Rat. Mech. Anal.*, **100** 13-52.

[7] Batthacharya, K. and Kohn, R. V. (1996) Symmetry, texture and the recoverable strain of shape memory polycristals , *Acta Meatll. et Materialia*, **44** 529-542.

[8] Brinson, L. C. (1993) One dimensional constitutive behavior of shape memory alloys:thermomechanical derivation with non-constant material functions, *J. Intell. mater. Syst & Struct.*, **4** 229-242.

[9] Coleman, B. D. and Noll, W. (1963) The thermodynamics of elastic materials with heat conduction and viscosity, *Arch. Rational Mech. Anal.*, **13** 167-178.

[10] Cristescu, N. and Suliciu, I. (1982) *Viscoplasticity* , Martinus Nijhoff Publishers, The Hague/ Boston/ London.

[11] Ericksen, J. L. (1975) Equilibrium of bars, *J. Elasticity*, **5**, 191-201.

[12] Falk, F. (1980) Model freee energy, mechanics, and thermodynamics of shape memory alloys, *Acta Metall. et Materialia*, **28**, 1773-1780.

[13] Făciu, C. (1985) On thermodynamic restrictions for the Navier-Stokes-Fourier fluids, *Stud. cerc. Mat.*, **37**, 447-456.

[14] Făciu, C. (1991) Numerical aspects in modelling phase transitions by rate-type constitutive equations. *Int. J. Eng. Sci.*, **29**, 1103-1119.

[15] Făciu, C. (1996) Initiation and growth of strain bands in rate-type viscoelastic materials. Part I: Discontinuous strain solutions. Part II: The energetics of the banding mechanism. *Eur. J. Mech. A/Solids*, **15**, 969-988, 989-1011.

[16] Făciu, C. and Suliciu, I. (1994) A Maxwellian model for pseudoelastic materials, *Scripta Metall. Mat.*, **31**, 1399-1404.

[17] Făciu, C. and Mihăilescu-Suliciu, M.(1987) The energy in one-dimensional rate-type semilinear viscoelasticity. *Int. J. Solids Structures*, **23**, 1505-1520.

[18] Făciu, C. and Mihăilescu-Suliciu, M. (2002a) On modelling phase propagation in SMAs by a Maxwellian thermo-viscoelastic approach, *Int. J. Solids Structures*, **39**, 3811-3830.

[19] Făciu, C. and Mihăilescu-Suliciu, M. (2002b) On a rate-type thermo-mechanical model for shape memory bars. Stress-controlled problems. *ZAMP* (in press).

[20] Făciu, C. and Mihăilescu-Suliciu, M. (2002b) Shape memory effect: a Maxwellian rate-type constitutive approach, Proceedings of NATO Advanced Research Workshop, "New Trends in Phase Transformatios and their Applications to Smart Structures, April 23-26, 2002, Metz. (Kluwer Academic Publisher).

[21] Grenet, J. and G'sell, C. (1990) Observation and modelling of shear-band propagation in glassy polycarbonate, *Polymer*, **31**, 2057-2065.

[22] James, R.D. (1981) Finite deformation by mechanical twinning. *Arch. Rational Mech. Anal.*, **77**, 143-176.

[23] James, R.D. (1983) Dispalcive phase transformation in solids .*J. Mech. Phys. Solids*, **34**, 359-394.

[24] Lin P.H, Tobushi H., Tanaka, K., Hattori, T. and Ikai, A. (1994) Influence of strain rate on deformation properties of TiNi shape memory alloy. *Trans. Jpn. Soc. Mech. Eng (A)*, **60**, 1837-1842.

[25] Leo, P.H., Shield, T. and Bruno, O.P. (1993) Transient heat transfer effects on the pseudoelastic behavior of shape memory wires. *Acta Metall. Mater.* **41**, 2477-2485.

[26] J. C. Maxwell (1879) On stresses in rarified gases arising from inequalities of temperature, *Trans. Roy. Soc. London*, **170**, 231-256.

[27] Mihăilescu-Suliciu M. and Suliciu I. (1993) Stable numerical solutions to a dynamic problem for a softening material, *Mech. Res. Comm.*, **20**, 475-480.

[28] Molinari, A., and Clifton, R.J., (1987) Analytical characterization of shear localization in thermovisco-plastic materials solids, *J. of Applied Mechanics*, **54**, 806-812.

[29] Otsuka, K. and Wayman, C.M. (Eds.) (1998) *Shape Memory Materials*, Cambridge University Press.

[30] Otsuka, K., Wayman, C. M., Nakai, K., Sakamoto, H. and Shimizu K. (1976) Superelasticity effects and stress-induced martensitic transformations in Cu-Al-Ni alloys, *Acta Metall. Mater.*, **24**, 207-226.

[31] Pego, R. (1987) Phase transitions in one-dimensional nonlinear viscoelasticity: admissibility and stability., *Arch. Rat. Mech. Anal.*, **97**, 353-394.

[32] Perkins, J. (Ed), (1975) *Shape memory effects in alloys*, Plenum Press.

[33] Rajagopal, K. R. and Srinivasa, A. R. (1995) On the inelastic behavior of solids - Part I: Twinning; Energetics associated with discontinuous deformation twinning, *Int. J. Plasticity*, **11**, 653-678.

[34] Shaw J. A. and S. Kyriakides, (1995) Thermomechanical aspects of NiTi, *J. Mech. Phys. Solids*, **43**, 1243-1281.

[35] Shaw J. A. and S. Kyriakides, (1997) On the nucleation and propagation of phase transformation fronts in a NiTi alloy, *Acta Mater.*, **45**, 683-700.

[36] Shaw J. A. and S. Kyriakides, (1998) Initiation and propagation of localized deformation in elasto-plastic strips under uniaxial tension, *Int. J. Plasticity*, **43**, 837-871.

[37] Shaw J. A., (2000) Simulations of localized thermo-mechanical behavior in a NiTi shape memory alloy, *Int. J. Plasticity*, **16**, 541-562.

[38] Shaw J. A. and S. Kyriakides, (1995) Thermomechanical aspects of NiTi, *J. Mech. Phys. Solids*, **43**, 1243-1281.

[39] Suliciu, I. (1983) On the shape memory alloys and the rate-type constitutive equations, Paper presented at Euromech Colloquium **171**, August 25 -September 3, 1983, Jablona, Poland (unpublished)..

[40] Suliciu, I. (1989) On the description of the dynamics of phase transitions by means of rate-type constitutive equations. A model problem. In *Plasticity '89*, (Eds. A.S. Khan and M. Tokuda), 417-420, Pergamon Press.

[41] Suliciu, I. (1992) Some stability-instability problems in phase transitions modelled by piecewise linear elastic or viscoelastic constitutive equations, *Int. J. Engng. Sci.*, **30**, 483-494.

[42] Suliciu, I. (1998) Energy estimates in rate-type thermo-viscoplasticity, *Int. J. Plasticity*, **14**, 227-244.

[43] Tanaka, K., Kobayashi, S. and Sato, Y. (1986) Thermomechanics of transformation pseudoelasticity and shape memory effects in alloys, *Int. J. Plasticity*, **2**, 59-72.

[44] Vainchtein A. (2002) Dynamics of non-isothermal martensitic phase transitions and hysteresis, *Int. J. Solids Structures*, **39**, 3387-3408.

[45] Vainchtein A. and Rosakis P. (1999) Hysteresis and stick-slip motion of phase boundaries in dynamic models of phase transitions., *J. Nonlinear Sci.*, **9**, 697-719.

[46] Ward, I. M. and Holliday L. (1975) A general introduction to the structure and prpperties of oriented polymers, In *Structure and Properties of Oriented Polymers*, Ed. Ward I. M. pp. 1-35, John Wiley and Sons, New York-Toronto.